

## ABSTRACT

### ADAPTATION OF THE BALLISTOSPORE DISCHARGE MECHANISM AMONG POROID AGARICOMYCETES

by Yunluan Cui

Most poroid basidiomycetes produce spores in vertically aligned fertilized hymenia in the form of tubes. The violently discharged spores must be propelled over limited distances to avoid impaction on the opposing surfaces of the tubes. Based on the widely accepted spore discharge model, we aim to find the keys that control the spore discharge distance, in order to reveal how ballistospores are adapted to the wide range of tube sizes. The study involved the use of a high-speed video camera to record the spore discharge process, and morphological studies of the basidiospores using scanning electron microscopy. Our models suggest that the size of Buller's drop, irrespective of spore size and mass, is the primary determinant of discharge distance. Meanwhile, the diverse morphology of ballistospores plays an important role in determining the final size of Buller's drop.

ADAPTATION OF THE BALLISTOSPORE DISCHARGE MECHANISM  
AMONG POROID AGARICOMYCETES

A Thesis

Submitted to the  
Faculty of Miami University  
in partial fulfillment of  
the requirements for the degree of  
Master of Science  
Department of Botany

By

Yunluan Cui

Miami University

Oxford, Ohio

2009

Advisor \_\_\_\_\_  
Nicholas P. Money

Reader \_\_\_\_\_  
Richard C. Moore

Reader \_\_\_\_\_  
M. Henry H. Stevens

## TABLE OF CONTENTS

CHAPETER	Page
1. INTRODUCTION	1
1.1 Background on Agaricomycetes	1
1.1.1 Poroid Agaricomycetes Diversity	2
1.1.2 Basidium Development	3
1.1.3 Morphology and Diversity of Basidiospores in Poroid Fungi	4
1.1.4 Introduction to Polypores Used in the Research	5
1.2 Hypotheses of Spore Discharge Mechanisms	6
1.2.1 Jet Propulsion Mechanism	8
1.2.2 Turgid Cell Rounding-off Mechanism	8
1.2.3 Gas Bubble Explosion Mechanism	9
1.2.4 Electrostatic Propulsion Mechanism	9
1.2.5 Surface Tension Catapult Mechanism	10
1.3 Dispersal of Basidiospores in Tubes	11
1.4 Significance of the Research	12
2. MATERIALS AND METHODS	14
2.1 Organisms	14
2.2 Microscopy	14
2.2.1 Ultra-high-speed Video and Conventional Video Microscopy on Spore Discharge	14
2.2.2 Spore Morphology Studies with Scanning Electron Microscopy	15
3. HYPOTHESES AND MATHEMEDICAL MODELING	17
3.1 Slight Effect of the Spore Size on the Discharge Distance	17
3.2 Involvement of Buller's Drop in Determining Spore Discharge Distance	18
3.3 Hypothesized Factors Affecting the Size of the Buller's Drop	19

4. DATA ANALYSES AND RESULTS	21
4.1 Data Obtained from Conventional Video and Ultra-high-speed Video	21
4.2 Development Rate of the Buller's Drop	22
4.3 Ballistospore Morphology	23
5. DISCUSSION	24
5.1 Spore Morphology and the Size of the Buller's Drop	24
5.2 Evolutionary Trend between the Spore Size and the Pore or Tube Sizes	25
REFERENCES	27

## LIST OF TABLES

	Page
1. Ballistospore discharge in three polypores	33
2. Sizes of spores and hilar appendix in three polypores	33

## LIST OF FIGURES

	Page
1. Diverse hymenophore structures in <i>Ganoderma applanatum</i> , <i>Pycnoporus cinnabarinus</i> , <i>Trametes hirsuta</i> , <i>Laetiporus sulphae</i> , <i>Trametes versicolor</i> , and <i>Ganoderma lucidum</i>	34
2. Basidia bearing ballistospores in <i>Polyporus squamosus</i> and b, <i>Polyporus badius</i>	35
3. Morphology of six polypore species	36
4. Spore discharge process in <i>Polyporus squamosus</i>	37
5. The process of ballistospore shedding from sterigma	38
6. Pathway of spores after discharge from the inner surface of tubes in a poroid fruiting body	39
7. Relationship between the pore diameter and the wall thickness	40
8. Relationship between the spore volume and the tube size	41
9. 3-D image showing the relationship between the spore sizes, the Buller's drop sizes, and the spore discharge distance	42
10. Effects of spore morphology on the development of Buller's drop	43
11. Development rate of the Buller's drop in <i>Polyporus squamosus</i>	44
12. Scanning electron micrographs of spores and basidia	45
13. Successive images showing spore discharge in <i>Trametes versicolor</i>	47
14. Deposit of spores along the inner side of the tubes in <i>Trametes versicolor</i>	48

## APPENDICES

	Page
Appendix A. Development of a typical basidium	49
Appendix B. Different types of mature basidia	50
Appendix C. Scanning electron micrograph showing the structure of a ballistospore in <i>Coprinus cinereus</i> : Agaricomycotina	51
Appendix D. Subdivision in Basidiomycotina	52

## ACKNOWLEDGEMENT

I would like to give my deepest thanks to my advisor Dr. Nicholas P. Money for his patience and warm heart during my master's research. He has had a great impact on me during my graduate program so far, as well being a scientific mentor and motivator. His professional guidance and encouragement allowed me to feel confident to voice my ideas and opinions about the project.

My sincere thanks are also provided to my committee members, Dr. M. Henry H. Stevens and Dr. Richard C. Moore. Their constant support has allowed me to achieve my research goals. Dr. M. Henry H. Stevens selflessly donated his time towards helping me with the statistical analyses. Dr. Mark W. F. Fischer, from College of Mount St. Joseph in Cincinnati, also contributed substantial guidance and brought his perspective and mathematical models to my work. More importantly, the scientific insights and discussions of all the faculty members in my research area greatly improved the completion of this document.

Without the support from the faculties, staffs, and students in Department of Botany, I would not have been able to complete my work. I would especially like to thank Jessica L. Stolze-Rybczynski for her amazing help and teaching me how to use the high-speed-video camera and analysis software. Meanwhile, during this project, I learned a lot about electron microscopy from Dr. Richard E. Edelman and Mr. Matt Duley, who are very experienced in this field, and thank them a lot for all their technical assistance to teach me how to use the scanning and transmission electron microscope.

Finally, but most importantly, I would like to thank my parents for their unlimited love to support me to study abroad in America. They encouraged me to go after my dreams, and gave me the confidence to achieve them. My lovely sister gave her endless care about my study and life in American, which also motivated me a lot during my research.

I am indebted to the people and organizations that ensured the financial support for this research. Major funding was provided through NSF award 0743074 (to NPM and Diana J. Davis) and the Academic Challenge Program in the Department of Botany, Miami University.

# Chapter 1 Introduction

## 1.1 Background on Agaricomycetes

The fungi kingdom represents a large group in the global ecosystem, and at this time, 70,000 species have been recorded, and new species are still added to update the list (Hawksworth, 1991). As the second largest group of fungi, the Basidiomycota alone consists of 30,000 species, ranked after the Ascomycota, and includes the most diverse fungi in the world (Kirk *et al.*, 2001). The long history of the group is traced back to the Late Devonian, when definitive Basidiomycota fossils were found. The Basidiomycota is further divided into three subphyla: Pucciniomycotina, Ustilaginomycotina, and Agaricomycotina, all of which are characterized by the basidium, a spore-bearing cell. The first two subphyla include the most familiar plant pathogens, causing corn rust and wheat smut. The Agaricomycotina are featured by the hymenia consisting of a layer of basidia under the fruiting bodies, which develop either not enclosed or only with a veil. Three classes in Agaricomycotina include the Agaricomycetes, Dacrymycetes, and Tremellomycetes. The tissue layer of basidia called hymenia under the fruiting bodies of the mushroom-forming fungi develop either not enclosed or only with a veil. Translucent jelly fungi and many yeast-forming species are in the clades of the Dacrymycetes and Tremellomycetes (Hibbett, 2007). The remaining 98% of the 20,000 recorded species in Agaricomycotina belong to Agaricomycetes, which include common mushrooms, bracket fungi, puffballs, and others (Hibbett, 2007). All the members of the clades are characterized by the production of basidiocarps, a multicellular structure on which the hymenium is borne. The size ranges from a few millimeters across to greater than one meter across (Gilbertson and Ryvarden, 1986). Though species share common characteristics, many have their own unique characteristics in terms of shape, color, and size. Further classification into orders includes Polyporales, Boletales, Agaricales and other mushroom-forming fungi.

The diverse patterns of fruiting bodies of Agaricomycetes are unmatched by other fungi, including poroid fungi, gilled fungi, tooth fungi, coral fungi, and crust fungi. The caps (i.e., pileus) usually take on a form of umbrella, bell, conical or convex, and others are bracket-shaped

or crustlike resupinate forms, which may be supported by central or off-center stalks of different length, or are unstalked. Fertilized hymenial tissues underneath the cap are organized in different ways to give diverse patterns of tubes (Polyporales), gills (Agaricales), teeth (Cantharellales), and some directly exposed to the air. For example, *Auriscalpium vulgare* has a toothed hymenium; *Fomitopsis pinicola* is a poroid bracket fungus; *Philebia chrysocra* appears in a resupinate form; and *Ramaria botrytis* takes on a coral form. The morphological diversity fully reflects that Agaricomycetes have evolved in multiple directions.

### 1.1.1 Poroid Agaricomycetes Diversity

The polyporales (earlier known as Aphyllophorales) are a large group in basidiomycetes, and evolved in polyphyletic direction (Hibbett and Donoghue, 1995; Binder and Hibbett, 2002). The habitats of poroid Agaricomycetes extend widely; many species develop on wood and lack fully developed stems; the fruiting bodies are shelf-like or crust-like, while some have more or less central stems and grow at the base or on the trunk of trees, and a few appear to develop on soil. Viewed from an ecological perspective, Polyporales play an important role as pathogens and wood decomposers, for example, *Meripilus giganteus*, is parasitic on living hardwoods and saprobic on the dead hardwoods, causing rot (Bessette, *et al.*, 1997).

The shape of the pores and their sizes are of taxonomic importance. The sizes of the fruiting bodies range from the tiny and invisible microfungi to the rampant and giant *Meripilus giganteus*, which can reach 30 cm in width (Larsen and Lombard, 1988). Instead of the soft lamellae (spore-bearing gills beneath the fruiting body) produced in gilled mushrooms, spores of Polyporales are produced in tubes. Tubes are packed tightly or loose, and the texture of the fruiting body is woody or soft. Their pore surface looks rather like the surface of a sponge. When taking a close look at the pored-hymenia underneath the cap of poroid Agaricomycetes, you may find some tubes are tightly packed, nearly invisible; others are discernable with the naked eye. For example, *Ganoderma applanatum*, the artist's bracket, has a pored surface with 4-6 regularly circular tiny pores per millimeter, invisible to the naked eye (but its cap, on the contrary, can reach 75 cm in width). *Polyporus squamosus* usually have distinguishable pores. For most species the number of pores per millimeter is a rather consistent character, although the

pores often have a tendency to become larger with age in some large fruiting-body species. Not all the pores are regularly round, the pore surface; hymenophores varies greatly among different species (Figure 1). Not all species have consistently round pores; hymenophore in some species may change with age and development. Besides the round or angular pores, a remarkable exception is the gilled polypore, *Lenzites betulina* and *Polyporus elegans*. Meanwhile, the depth of tubes and the wall thickness also vary from species to species; tube length changes in the range from no more than one millimeter to several centimeters.

### **1.1.2 Basidium Development**

The basidium is a terminal cell of the hyphae, constituting the fertile tissue on the underside of the pileus of the fruiting body. Basidia are aligned horizontally along the inner surfaces of the tubes (Figure 2). For coral fungi, basidia align in a continuous layer covering the surfaces of the erect coral branches. Most of the mushrooms produce spores on the exterior of the microscopic club-shaped basidia, which in contrast with the endogenous spores of the ascus bear spores exogenously. During the development of the basidia, a unique hyphae growth pattern occurs at the tip of fertile hyphae under the cap, and results in a swollen basidium, dominated by numerous vacuoles (Appendix A). Before long, four teeth-like structure called sterigmata grow protruding out of the top of the basidium. When basidia reach their maturity, each spore initial is formed by inflation of the apex of a single sterigma, followed by the formation of a tiny ball-shaped structure. Gradually, the structures enlarge and develop into spores. Meiosis occurs and gives rise to four nuclei. As the result of the migration of the four nuclei, each nucleus is distributed into one basidiospore and result in uninucleate basidiospores. Fully developed spores are full of cytoplasm, and the body of the basidium contains an enlarged vacuole surrounded by a layer of cytoplasm, therefore, connection between spores and basidium is through direct cytoplasmic continuity (Ross, 1979). There is a great variation in morphology of the basidium, the number of spores it supports, and the way the spores attach to the basidium. Exceptions to this developmental model include the direct attachment of spores to the basidium without sterigmata and the production of less than four spores in some basidia. Two-spored basidia are also common, and in some species such as the stinkhorn (Order Phallales, Class Agaricomycetes), each basidium may support as many as nine spores (Ingold, 1998) (Appendix B).

### 1.1.3 Morphology and Diversity of Basidiospores in Poroid Fungi

The short oblique protrusion called the hilar appendix is located at the narrow end near the base of the spore is a unique structure of basidiospores. On the tips of four minute sterigma, four spores are poised asymmetrically, each having an attachment region on its surface that functions to anchor it to the sterigmata. Usually, the adaxial or dorsal face is less strongly curved than the abaxial or ventral face, and it contributes to the bilateral symmetry of the spore. The hilar appendix, an extended, slightly curved part of basidiospores, is the site of formation of the Buller's drop (Buller, 1922). This specialized structure on the proximal end of the spore is of different lengths, and the angle between it and the spore are not the same between species. As the spore matures, successive wall layers are deposited. The cross section and longitudinal section of the spore reveal the area next to the hilar appendix is much thinner, and it is the region where an important droplet (Buller's drop) originates (Appendix C).

As with the diverse appearance of the fruiting bodies, spores develop in various manners resulting in different sizes and structures. Spore volumes also change significantly, from  $2.0 \times 10^{-15} \text{ m}^3$  to  $1.8 \times 10^{-14} \text{ m}^3$  (Gilbertson and Ryvarden, 1986, 1987). The basidiospores typically range in form from spherical, to oblong, ellipsoid and cylindrical. In most cases, the surface of the spore can be fairly smooth, but in a limited number of genera, the spores are ornamented to varying degrees with small warts, or spines (Gilbertson and Ryvarden, 1986). Different spore surface structures are presented in many fungal species as unique classification characters: for example, species of *Ganoderma* are characterized by thick-walled spores with regular pattern of warts or protuberances, making the spores very distinctive; spores of *Boletopsis smithii* are angular, with 4-6 tubercles; *Boletopsis subsquamosa* spores are irregular in outline; *Bondarzewia berkeleyi* spores are ornamented with short, irregularly arranged, strongly amyloid ridges; oblong spores in *Coltricielle dependens* have a prominent apiculus; and the outer wall of basidiospores in species *Ganoderma lucidum*, *Ganoderma oregonense* and *Ganoderma tsugae* have pronounced depressions and appear rough (Gilbertson and Ryvarden, 1986). Though the shape and size of the basidiospores differ greatly between species, within a single species they show little variation.

#### 1.1.4 Introduction to Polypores used in the Research

The types of basidiocarps favored by natural selection are those that could offer fertile tissue protection from loss of moisture. Establishment of highly ordered hymenium, as the gills, pores, or tubes reduce the exposure of the hymenium, helps maintain a higher humidity and enhances spore production (Thiers, 1984). Therefore, we focus on the poroid fungi to explore the potential relationship between spore discharge mechanism and the sizes of enclosed hymenium tubes.

In my research, six common polypore species were used, including *Ganoderma applanatum*, *Trametes elegans*, *Polyporus badius*, *Polyporus squamosus*, *Trametes versicolor* and *Cerrena unicolor* (Figure 3). They are in family of Polyporaceae and Ganodermataceae (Appendix D). The spore size, pore size and the size of basidiocarps in these polypores change greatly, making them great choice for morphologic study. Meanwhile, the fertile tissue is easy to manipulate to be used in the microscopy, which facilitated the capture of spore discharge process.

*Polyporus squamosus* have relatively largest spores in the six polypores and the pore shape is irregular. This bracket fungus commonly grows alone or more typically in clusters of two or more fruiting bodies on decaying hardwood. They are found in spring, and sometimes in summer and fall. Generally, the fruiting body is 5-30 cm across and up to 4 cm thick (Gilbertson and Ryvarden, 1987). The spore is broadly ellipitical to oblong, with minor width 10-16  $\mu\text{m}$  and major width 4-6  $\mu\text{m}$  (Lincoff, 1992; Phillips, 1991, 2006).

*Ganoderma applanatum*, known as Artist's fungi, grow scattered or in overlapping clusters on decaying wood. This year-round woody and shelf-like polypore has a wide stalkless cap, which can reach 65 cm in diameter. There are 4-6 circular pores per millimeter. Spores are broadly elliptic, truncated with a thick double wall with major and minor width 7-11 $\mu\text{m}$  and 5-7.5  $\mu\text{m}$ , respectively (Bessette, 1997).

*Trametes elegans*, this maze polypore is easy to recognize by the changes of the pore surface from the base to the margin. The cap is leathery to corky when fresh, becoming stiff when dry. Pore surface changes from white to pale in age. The shape of the pore highly varies, typically

labyrinthine, gill-like or poroid, usually 1-2 irregular pores per millimeter. Spores are cylindrical with a major width of 5-7 $\mu$ m and minor width 2-3  $\mu$ m (Bessette, 1997).

*Polyporus badius*, also called black-footed polypore, is a small, centrally stalked polypore. The fruiting bodies are fairly common through August to December. They grow in groups or scattered on decaying hardwood. Caps are typically funnel-shaped with a smooth shiny surface. Stalks are long, thick and smooth, and color changes from reddish brown near the apex to black below. Pore surface is white, with 5-7 tiny pores per millimeter. Spores are 6-10  $\mu$ m in major width and 3-5  $\mu$ m in minor width (Bessette, 1997).

*Trametes versicolor*, known as "turkey tail", is all year-round, and is a widely distributed common mushroom in North American woods, found virtually anywhere on dead hardwood logs and stumps (Gilbertson and Ryvarden, 1987; Barron 1999). This saprobic fungus grows in dense, overlapping clusters or rosettes on dead logs and stumps. The pore surface is whitish to pale grayish, with tiny pores around 4 or more per mm. Tubes reach up to 3 mm deep. The minor and major width of the smooth and cylindrical spore is 5-6 $\mu$ m in major width and 1.5-6  $\mu$ m in minor width.

*Cerrena unicolor*, commonly known as the "mossy maze polypore", is a little saprobic polypore that grows in overlapping clusters. It is year-round and causes a white rot on logs. Kidney-shaped to fan-shaped caps can reach 3-10 cm across. Maze-like pore surface becomes tooth-like with age. The velvety to hairy upper surface is whitish to grayish, and sometimes green from algal growth. It is attached to the growing surface without a stalk. Elliptical shaped spores have dimensions of 5-7  $\mu$ m x 2.5-4  $\mu$ m in minor and major diameters (Barron, 1999; Gilbertson and Ryvarden, 1987; Lincoff, 1992).

## **1.2 Hypotheses of Spore Discharge Mechanisms**

Among the basidiomycete species, the widely accepted spore discharge mechanism is described as the surface tension catapult. It explains the dynamic mechanism involved in the violent spore discharge process. In poroid Agaricomycetes, understanding how this mechanism is related with

diverse fruiting body forms and spore morphology will provide important insights into the biology of these fungi.

Basidiospores can be released positively or negatively. Basidiospores that are propelled by the violent spore discharge mechanism are ballistospores. They typically involve the sudden release of the surface tension, and the abrupt change of center of gravity on the spore. Most species retain their violently forcible discharge mechanism, and spore release is caused by fluid movement over individual spores, rather than the external assistance as described above. Other basidiospores are not characterized by forcible discharge, however, and are ejected by external force or vectors. Stinkhorns depend on insect vectors; puffballs require external force to release dried spores efficiently; bird's nest fungi use the splash-cup mechanism to disperse spore-containing structures by rain; and earthballs rely on the disturbance of basidiocarps. Though these groups have lost the forcible discharge mechanism along their evolutionary course, they still form basidiospores. In these cases, the basidiospores typically lack a hilar appendix, and there is no Buller's drop formation. This diversity among discharge processes demonstrates independent evolutionary direction of the forcible discharge mechanisms ancestral to all basidiomycetes. The mechanisms of basidiospore discharge still have not been achieved agreement. It is possible that one mechanism plays a dominant role in some cases, and is assisted by other mechanisms. Based on most observation of basidiomycete spores before their discharge, a surface tension catapult involved with the formation of Buller's drop seems to be the major mechanism to explain how the basidiospores are launched.

Fungal spores serve as reproductive units, and are dispersed in the air. Spore types are diverse and complex in the fungi depending on the species, habitat, and life history, but polypores primarily rely mostly upon unicellular haploid basidiospores. These airborne spores have a unique way to be launched from their parents into a new habitat. In the reproductive season of basidiomycetes, billions of spores are produced and released in a single day from a single mushroom (Buller, 1909; Kramer, 1982). To increase the reproductive success of the spores, it seems necessary to ensure that spores are released from the hymenium and escape from the tubes before they randomly land. Basidiospore dispersal in the Agaricomycetes fully demonstrates the various spore discharge mechanisms among the fungi. Fungal spores may be released actively

by mechanisms both chemical and physical, reflecting the genetic information of different fungi. Once released, they are carried away by wind or animals. As recorded in *Biology of the Fungi* (Ross and Ian, 1979) and *Introduction to Fungi* (Webster, 1980), there are five ways that basidiospores are hypothesized to be actively released.

### **1.2.1 Jet Propulsion Mechanism**

One spore release mechanism proposed by Brefeld (1877), Corner (1948), and Muller (1954) is jet propulsion. They proposed that the projection of basidiospores was similar to that of *Pilobolus*, by the bursting of a turgid cell (mainly occurring in Ascomycetes and some Zygomycetes). In this case the increasing turgor pressure inside the basidium accumulates and inflates the sterigmata. Turgor pressure reaches its maximum level after spores mature, creating a tightly blown-up structure. When environmental factors change, a rupture around the turgor-filled sterigma results in an explosive release of pressure in the form of a jet of cell sap through the tips, which pushes the spore over a certain distance. The squirting gun suddenly projects spores in the form of projectiles flying through the air. This spore discharge method releases the spores violently, and can launch the spores far away from the fruiting body. However, if this is the case, there are some unexplainable phenomena. First, the sterigmata and basidium should shrink to some extent, or there should be some detectable changes in the volume of the basidium. Actually, observation shows that successive spore discharges do not deform the basidium and the sterigma. Another objection against this assumption is that maintenance of the basidial turgor to propel newly formed spores requires the tip of sterigma to seal off following spore discharge. There is no evidence of a pore shown in the electron micrographs of the sterigmata after spore detachment (Webster, 1980).

### **1.2.2 Turgid Cell Rounding-off Mechanism**

The rounding-off of turgid cells occurs in some zygomycetes and basidiomycetes. Ingold (1971) discussed the liberation of spores by the rounding-off of a turgid cell as a forcible spore discharge mechanism in a variety of different genera (Mims and Richardson, 2005). This mechanism is characterized by a surface between the spore and sterigma under tension. Based

on the observation of the rust fungus *Gymnosporangium nidus-avis*, after the spores are released, both the hilum of the spore and the end of the sterigma are convex. Basidiospores bounce off the sterigma by rounding-off of both turgid secondary walls laid down on either side of the original septum. It is possible that the turgor pressure within the basidium contributes to the force that drives basidiospore discharge. Another example is *Sphaerobolus*, also a basidiomycete species, whose spore-producing structure is enclosed by several layers of sterile tissue in a cup-shape. At maturity, the highly osmotic concentrated layers absorb water and result in a progressively unstable situation as the turgor pressure of the inner part of the cup increases. Stress is relieved by a sudden eversion of the inner cup to project the spores, taking advantage of rapid motion (Webster, 1952).

### **1.2.3 Gas Bubble Explosion Mechanism**

The concept of explosive discharge mechanism was proposed by Olive (1964), who suggested that there is a gas bubble located at the junction of the sterigma and the spore apiculus. The small gas bubble explosion and residual gas accumulated between the inner wall and outer membrane of the spore results in the ejection of the ballistospores. This was also supported by Ingold and Dan (1968), who found fewer spores were discharged when pressure higher than atmospheric pressure was applied when testing the effect of external gas pressure on spore discharge. Other evidence comes from electron micrographs showing the circular rupture of the spore in the position occupied by the gas bubble, and the calculated value of the power the gas jet should possess to project the spore. However this mechanism was rejected by Savile (1965) and Van Niel (1972), who verified that the bursting force could not result in the appropriate discharge direction of the basidiospores.

### **1.2.4 Electrostatic Repulsion Mechanism**

The most bizarre one among the diverse mechanisms proposed is electrostatic repulsion. The experiment that favored this hypothesis was described by Buller (1909) and Gregory (1957), who proposed that electrostatic charges were implicated in the discharge of basidiospores. It showed the majority of spores were prone to fall on one or another side of an electrostatically-charged

plate placed under the fruiting body. Therefore, the explanation could be proposed that the electrostatic repulsion between the spore and sterigma could be responsible for the spore projection. However, there is no data showing what magnitude of charge is adequate to permit the spores to escape from the fruiting body. Meanwhile, spores and sterigmata are continuous, if the gain in charge occurs at the moment they separate, then they should gain the same magnitude with the opposite charge, which will attract spores and sterigmata together, rather than repel. Therefore, the electrostatic repulsion mechanism should be rejected.

### **1.2.5 Surface Tension Catapult Mechanism**

Most basidiomycetes share a unique forcible mechanism of spore discharge. The mechanism described as surface tension catapult, is the main method to disperse the progeny from the parents and it dominates the basidiomycetes. As described by Buller (1922), ballistospores develop on the tips of the sterigmata of the basidium. Just before discharge, a droplet of fluid, called Buller's drop, begins to form and enlarges at the tip of the hilar appendix located at the base of each spore. At the moment of spore discharge, the Buller's drop will reach its final size, usually with a diameter approaching the spore width, and collapses onto the spore surface, fusing with a film of fluid called the adaxial drop, which causes a shift in mass toward the spore center, and suddenly and violently catapults the spore into the air (Pringle *et al.*, 2005) (Figure 5).

Droplet collapse is driven by surface tension. Ingold (1939) calculated the energy released by the sudden transformation of the spherical droplet to a hemispherical drop of water adhering to the spore and determined that this process provides sufficient energy need to drive the spore discharge. It is reported that released surface tension at coalescence imparts a significant momentum to launch spores at initial accelerations in excess of 10,000 g, and propels the spore up to 1 mm from the basidia. After discharge, spore velocity decreases rapidly because of the overpowering effect of air viscosity on spore motion, and the spore falls vertically through the tube interior (or between the gills), and is then blown far away from the fruiting body by air currents.

The unique ballistospore propulsion mechanism involves the growth of two droplets that function as critical condensation areas for water vapor from the air. They are located separately

on the pore surface, one on the base of the spore, at the pointed tip of the hilar appendix, the other on the adaxial surface of the spores above it. During the maturation of a basidiospore, sugars are exuded onto the cell wall as a hygroscopic material, which causes the water to condense upon it when the surrounding humidity is high enough. Mannitol and hexoses contribute significantly to the hygroscopic nature of Buller's drop in basidiomycetes (Webster *et al*, 1995). As a result, Buller's drop accumulates as a large, almost spherical water droplet supported by the hilar appendix. At the same time, condensation occurs in form of a thin film called the adaxial drop on the adaxial face of the spore. When these two bodies of water gradually grow larger enough, they make contact with each other and coalesce, and the release of surface tension and the sudden change in the center of mass leads to sudden discharge of the basidiospore, as described above (Figure 5).

Only one spore at a time is projected from each basidium, and several seconds may elapse between the discharges. It is reported by many investigators that no shrinkage occurs in the basidia and sterigmata until long after all spores have been shot off. The mature basidiospores are forcibly discharged in sequence from each basidium located on the exposed hymenium at maturity, and all four spores produced by any one basidium are projected the same distance.

### **1.3 Dispersal of Basidiospores in Tubes**

What happens to the spore after discharge determines its fortune. The hymenium develops uniformly on the lower side of the cap. In longitudinal sections, the hymenia are shown almost vertically in many basidiomycetes, and the basidia lie horizontally. The released spores are shot forward horizontally into the space between the hymenial tissues (Figure 6). Counteracted by the overwhelming air resistance, the speed of the discharged spore drops dramatically to zero after a certain distance along the launch direction. After a sharp right turn, spores fall vertically through the narrow spaces between the tissues until they reach the opening, where they are caught up and carried away by air currents. Depending on the size of the tube, the tilt angle of the fruiting body may influence the amount of spores that escape from the pileus. If the pileus is tilted, the discharged spores will be caught by the neighboring hymenium during descent. To be effective in the dispersal of spores, like the vascular plants, fungi show gravitropism to some

extent, though the response mechanism is unknown. Two species of agarics will respond to gravity when the stipes are oriented horizontally, and they gradually bend upward to adjust the position of the basidiocarp at the same time as the basidiospores achieve maturation (Kher *et al.*, 1992; Monzer *et al.*, 1994). This process involves the differential growth in the stipe, resulting from the faster growth in the lower side of the stipe. Therefore, the gills or tubes beneath the basidiocarp are always perpendicular to the ground, which assures the launched basidiospores can fall vertically through the tubes by gravity. Newly formed tissues of stipeless bracket fungus *Ganoderma applanatum*, always reorient themselves with the tubes perpendicular to the ground.

However, the space where the spores are launched is surrounded by hymenial tissue. Not all of the spores discharged from the basidia can reach the pore opening: on one hand, they should be launched over a certain distance to avoid the tissues beneath impeding their descent pathway; on the other hand, the spores should not travel too far to collide with the opposing tissues. Therefore, the spore discharge distance should be kept within a certain range in order to assure more spores have the chance to leave the mature fruiting bodies.

#### **1.4 Significance of the Research**

There is a tremendous variety of fruiting body morphology among the Agaricomycetes. No matter how the pores are arranged over the lower surface of the pileus, there is always a mechanism to control the spores to be launched over a proper distance, and to ensure the spores are released from the fruiting body. In mushroom-forming species (Agaricomycetes) with closely crowded tubes or pores, such as boletes and polypores, suppose that the hymenia are all vertically arranged, the basidiospores must be discharged within a limited range to avoid impaction on the opposing hymenial surfaces. It seems likely that if spore size is a major determinant of discharge distances that there would be a significant relationship between spore size and tube size in Agaricomycetes with poroid fruiting bodies. This project is concerned with adaptations to the ballistospore discharge mechanism among poroid basidiomycete fungi. Based on the surface tension catapult mechanism of basidiospore discharge, it provides an appealing project to explore whether any relationship exists between the spore size, the morphology of spores, and the tube size. It is possible that we might find several factors to benefit our

understanding on the significance of spore morphology in Agaricomycetes. My research aims to clarify the significance of ballistospore morphology in poroid Agaricomycetes.

## **Chapter 2 Materials and Methods**

### **2.1 Organisms**

Polypores are poroid Agaricomycetes and possess a pore surface, which is usually hard to peel from the cap. Six polypores studied in this research include *Polyporus squamosus*, *Polyporus badius*, *Ganoderma lucidum*, *Cerrena unicolor*, *Trametes elegans*, and *Trametes versicolor*. They all have a layer of tubes with different depth on the underside of the cap. *Polyporus squamosus*, *Cerrena unicolor* and *Trametes versicolor* could be found through late spring to late fall in the Miami Natural Areas, Oxford Ohio; *Polyporus badius*, *Trametes elegans*, and *Ganoderma lucidum*, were collected in late summer in Miami Natural Areas, Oxford Ohio.

Fruiting bodies of polypores were collected from various sites in Ohio where collecting permits were not required and were preserved in small coolers or wax bags when they were collected in the field. A wet paper towel was placed in the bags in order to maintain the humidity. Before taking videos, the basidiocarps were wrapped with wet paper towels, and stored in refrigerator to avoid basidium and spore dehydration. Usually the fresh mushrooms could be kept for 24 hours to guarantee that the observations were made on fresh materials.

### **2.2 Microscopy**

The size of the spore, as well as the initial speed after the spore discharge, is beyond observation with the naked eye. Therefore, high speed video microscopy techniques were used to study the Buller's drop formation and expansion, and scanning electron microscopy was used to observe the spore morphology.

#### **2.2.1 Ultra-high-speed Video and conventional Video Microscopy for Spore Discharge**

To record the speed of the spore discharge and the final size of Buller's drop, high-speed and conventional pixel video microscopy was used. Video recordings were made with FASTCAM-

ultima APX and APX-RS cameras (Photron, San Diego, CA) attached to an inverted compound microscope fitted with long-working distance objectives (Olympus, Tokyo). Each video clip was compiled from  $\leq 100$  image files extracted from recordings consisting up to 1 million images captured in  $\leq 4$  s (e.g., 1 million image files captured with 2  $\mu$ m shutter at 250,000 fps in 4 s). Analysis of digital images was performed using VideoPoint v.2.5 (Lenox Softworks, Lenox MA), Image-Pro Plus 6.2 (Media Cybernetics, Bethesda, MD), and proprietary software from Photron. To record the Buller's drop formation, PixelFly CCD (Cooke Corp. Romulus, MJ) was used. The camera recorded 23 fps that is 1 image every 43.5 ms. Images recording the final size of Buller's drop were extracted and processed using Image-Pro Plus 6.2.

To study Buller's drop formation, 0.5-1 mm slices of hymenium were cut from the underside of basidiocarps, placed in Petri dishes, and sealed with Parafilm. Successful discharge of basidiospores depends on an absence of free water but requires an atmosphere saturated with enough water vapor around the spores. Usually the Petri dishes were prefilled with a thin layer of distilled water agar, which helped to support the hymenium block, and maintain the moisture. Meanwhile, under the high intensity of light, proper humidity could be maintained by placing a moist tissue paper circling the inside of the Petri dish, in order to prevent the tissue from drying.

## **2.2.2 Spore Morphology Studies with Scanning Electron Microscopy**

### **Hymenial Tissue Preparation**

Fertile tissues from fresh mushrooms at different stages of development were cut into 1-2 mm<sup>2</sup> slices. These were immersion fixed in glass vials with 2% paraformaldehyde and 2% glutaraldehyde in 0.05 M sodium cacodylate buffer with pH 7.0 for 3 hours at room temperature (Bozzola and Russell, 1998). The paraformaldehyde and glutaraldehyde crosslink the protein molecules in the cells to provide stability and the buffer prevents denaturing of the proteins (Bozzola and Russell, 1998). Following the primary fixation, tissues were washed in 0.05 M sodium cacodylate buffer four times at 15 min intervals, which gets rid of excess unreacted aldehyde remaining in the tissue. Postfixation was conducted in 1% osmium tetroxide for 1 h at room temperature. The osmium tetroxide could fix the lipids in the sample and also make the sample more conductive (Bozzola and Russell, 1998). After secondary fixation, the samples

were rinsed in distilled/deionized water four times at 15 min intervals. Finally, dehydration in a graded ethanol series (25%, 50%, 75%, 95% for 15 min each, and three times in 100% for 30 min intervals) was conducted according to standard dehydration protocol (Bozzola and Russell, 1998). The dehydration steps slowly replace all the free water in the sample. Critical point drying in liquid CO<sub>2</sub> was performed in a critical point dryer, in which liquid CO<sub>2</sub> replaced the ethanol and the samples remained structurally sound after drying. The samples were mounted with an adhesive on metal stubs, grounded with silver paint, coated with a 20 nm thick gold and viewed with scanning electron microscope Zessi Supra 35VP FEG at proper acceleration voltage (Bozzola and Russell, 1998).

### **Spore Preparation**

Spores were collected by preparation of spore prints. During spore collection, a block of mature hymenial tissue was placed horizontally in a Petri dish. To avoid the shrinkage of discharged spores, a film of the first fixative made of 2% paraformaldehyde and 2% glutaraldehyde in 0.05 M sodium cacodylate buffer (pH 7.0) was preloaded in the Petri dish under the tissue without contact. The Petri dish was set in room temperature for overnight, and then the spores were harvested with the first fixative.

Coverslips were rinsed repeatedly with ethanol and distilled water, and placed on parafilm in a Petri dish. A drop of the poly-L-lysine solution (1 µg/ml high molecular weight) was spread on a clean coverslip by drawing the edge of another coverslip over its surface. The coverslip was allowed to set for 15 minutes in a covered Petri dish. The coverslips were rinsed with double distilled water. A drop of the sample containing spores in the fixative was placed on the reactive surface. The spores were allowed to settle down on the surface for 1 hour. Samples were washed four times (15 minute intervals) in 0.05 M sodium cacodylate buffer (pH 7.0).

Coverslips were stacked in a coverslip holder for rinsing. Secondary fixation was conducted in 2% osmium tetroxide (OsO<sub>4</sub>) for two hours. Samples were then washed four times (15 minutes intervals) in distilled/deionized water in the cover slip holder. Standard dehydration in a grade series of ethanol and critical point drying in liquid CO<sub>2</sub> followed. The dried coverslips carrying the spores were mounted onto metal stubs, grounded with silver paint, and sputter coated with 20 nm gold.

## Chapter 3 Hypotheses and Mathematical Modeling

### 3.1 Slight Effect of the Spore Size on the Spore Discharge Distance

In the tubes, or between the gills of mushroom forming fungi, spores experience a significant air drag force immediately after discharge, and they decelerate dramatically due to the air resistance. In the Agaricomycetes with poroid basidiomes, my hypothesis is that spore size and discharge distance are related, with relatively large spores being launched over a long distance, and vice versa. When taking into consideration the air drag effects on movement of microscopic particles, it is logical to expect that with the same initial velocity, larger spores will tend to traverse greater distances than smaller ones (Money and Fischer, 2008). On one hand, for the same initial velocity, larger spores possess higher kinetic energy ( $F=mv^2$ ), and on the other hand, they are subject to relatively slight influence by air drag. Therefore larger spores experience less deceleration than smaller ones, and may tend to traverse greater distances (Money and Fischer, 2008). If discharge distance is related to the width of opening of the tubes, then it is reasonable to propose that species bearing wider tubes will tend to produce larger spores.

To test this hypothesis, we mined published taxonomic data from Gilbertson and Ryvardeen (1986, 1987), and used the data to examine the statistical relationship between spore sizes (or mass) and tube diameters. The sizes of the tubes or pores under the basidiocarp were indirectly described as the pore density: the number of pores along one dimension per millimeter. Six basidiomycetes species with poroid hymenophores were used to test the relationship between the wall thickness and the pore diameter (Figure 7). In 95% confidence intervals,  $r^2$  equals 0.83. Therefore based on the graph, we assumed pore diameter and the wall thickness are proportional, and high density correlated with small pore size. To simplify the calculation, we assumed all the spores to be standard ellipsoids. Based on 237 species of polypores with poroid fruiting bodies, the ordinary least-squares (OLS) regression shows larger spores are correlated with low dense tubes, and vice versa (Figure 8). We used SigmaStat (Windows Version 2.03 Build 2.03.0) to analysis the data and got the correlation coefficient 0.307. However, the data are so scattered in the graph, which indicates that spore volume has faint relationship with tube radius, unable to

explain the expected positive correlation between average tube radius and spore volume.

### 3.2 Involvement of Buller's Drop in Determining the Discharge Distance

Although this association between spore size and tube width is consistent with our hypothesis, the relationship is very weak. There is a great deal of scatter, or noise, in our data. This suggests that other factors may control spore discharge distance in these poroid fruiting bodies. Based on the analysis of the catapult discharge mechanism, it is clear that Buller's drop provides the energy to launch the spores. The change of surface tension from the spherical Buller's drop to the hemisphere droplet riding on the spore immediately after the spore discharge provides the momentum. In order to test relationship between the size of the spores, Buller's drops, and discharge distances, we applied a model designed by Dr. Mark Fischer from the Department of Chemistry & Physical Science at the College of Mount St. Joseph in Cincinnati:

This is the expression for the x-position of the spore as a function of time:

$$x(t) = x_i + \frac{mv_i \text{Cos}(\theta)}{6\pi r \eta} - \frac{e^{-\frac{6\pi r \eta t}{m}} mv_i \text{Cos}(\theta)}{6\pi r \eta}$$

In the limit as t goes to infinity, this x-position becomes the *maximum* x position:

$$\text{Limit}_{x \rightarrow \infty} x(t) = x_{\max}$$

But we notice that the exponential term goes to zero:

$$\text{Limit}_{x \rightarrow \infty} e^{-\frac{6\pi r \eta t}{m}} = 0$$

Thus, we see that  $x_{\max}$  could be simplified to:

$$x_{\max} = x_i + \frac{mv_i \text{Cos}(\theta)}{6\pi r \eta}$$

We can invert this, solving for the initial velocity required to produce a specified  $x_{\max}$ :

$$v_i = (x_{\max} - x_i) \frac{6\pi r \eta}{m \text{Cos}(\theta)}$$

Based on the hypothesis that the energy for spore discharge is derived from the rapid movement of Buller's drop onto the spore surface, we set different sizes for Buller's drop. In most cases, the width of Buller's drop won't exceed the minor radius of the spore. Buller's drop collapses on the spore surface, to mix with the film of water, adaxial drop, or adheres to the spore to form a hemispherical droplet, and it is obvious that not all of its surface tension is released. It is necessary to estimate the net change in surface free energy associated with drop movement. Without volume changes, we can calculate the surface area of the hemisphere, and further obtain the surface tension difference, which is the energy to eject the spores. Usually only 20% released surface tension is used to launch the spores. The surface tension at an air-water interface at 20 C is  $7.28 \times 10^{-2} \text{ N m}^{-1} = 73 \text{ mJ m}^{-2}$ , therefore, the surface area of a Buller's drop with radius  $1.0 \text{ }\mu\text{m}$  possess the surface tension of  $0.92 \times 10^{-12} \text{ J}$ . The calculated working energy that launches the spores is  $0.38 \times 10^{-13} \text{ J}$ . Based on the formula:  $F = \frac{1}{2} mv^2$ , using *Polyporus squamosus* as an example, the total mass of the spore ( $5 \times 11 \text{ }\mu\text{m}$ ) and attached fluid is  $6.40 \times 10^{-13} \text{ kg}$  (spore density is regarded as  $1.2 \text{ kg m}^{-3}$ , and the droplet density is  $1.0 \text{ kg m}^{-3}$ ), and correspondingly, the discharge velocity could be calculated as  $0.34 \text{ m/s}$ . The discharge distance is calculated by using the spore sizes, and sizes of Buller's drop, and calculated velocity in Mark Fischer's mathematical model. Finally we plotted the distance of spore discharge with different Buller's drop sizes and spore sizes using SigmaPlot 10.0 software (Figure 9). We found that variation in drop size produces a wide range in discharge distance. Therefore, it demonstrates that the size of Buller's drop rather than the spore sizes that play a dominant role in determining the discharge distance: small volume change of Buller's drop will result in obvious distance changes, which reasonably explains the noise between the tube size and spore sizes (Figure 8).

### **3.3 Hypothesized Factors Affecting the Size of Buller's Drop**

Buller's drop originates at the base of a spore, and it is closely related with the size and shape of the ballistospore. Obviously, Buller's drop cannot enlarge indefinitely, and the volume increase is confined to a certain range. On one hand, there is a defined space available to allow the Buller's drop development between the spores on the same basidium; on the other hand, the spore morphology is also a limiting factor to restrict the final size of the Buller's drop.

Therefore, it is hypothesized that spore morphology affects the final size of Buller's drop. The belief that the size of Buller's drop likely determines the spore discharge distance completely depends on the fact that different spore morphologies provide great opportunities to influence the formation of Buller's drop (Figure 10).

A number of characteristics of spore morphology are considered to be important taxonomic features. If larger spores have a longer hilar appendix, this is able to provide more space to allow the drop development. The lunate or allantoid shaped spores possess higher asymmetry than the cylindrical or globose spores, and provide more available space for Buller's drop enlargement before it collapses on spore surface. By contrast, spherical spores may not be able to support a large Buller's drop, which would decrease the potential spore-launching energy. The angle between the hilar appendix and the spore, and the height of the hilar appendix all determine the final size of the Buller's drop. Consider spores with a short hilar appendix; in this case, the Buller's drop is very close to the adjacent spore surface, and it would not grow large before it coalesces with the adaxial drop. The surface ornamentation (spikes or verrucae) is another limiting factor on the final size of Buller's drop. For example, long ridges would limit the expansion of Buller's drop. It is reported that in some species there is an area situated above the hilar appendix on the adaxial side of spore, called suprahilar disc, which is smooth in some species and roughened in others. The suprahilar disc provides more space for Buller's drop enlargement. In this case, the drop could grow larger before it contacts the adaxial drop.

In the following chapter, I describe the test the hypotheses gathered from the mathematical model, with the aim of identifying those factors that affect the spore discharge mechanism, and to determine how they function to determine the spore discharge distance.

## Chapter 4 Data Analyses and Results

### 4.1 Data Obtained from Conventional Video and Ultra-high-speed Video

We used ultra-high-speed video microscopy to record the spore discharge process. Each video clip recording spore discharge was compiled from less than 40 images files extracted from recordings consisting up one million images captured in 4 s. Each video clip recording the Buller's drop formation was compiled from 100 - 200 image files extracted from recordings consisting up to 351 images captured in 15 s.

The launch of the spores is powered by the energy released from formation and collapse of Buller's drop into the adaxial drop on the spore surface (Table 1). The recorded initial discharge velocity varies in the three polypores species, from 0.58 m/s to 0.68 m/s with *Trametes versicolor* discharging at the highest speed. Though the range of mean discharge speed is limited, the measured discharge distance takes on a 4-fold increase, from 0.03 mm in *Trametes versicolor* (smallest spore) to 0.13 mm in *Polyporus squamosus* (largest spore). Greater discharge distance correlated with larger spores and Buller's drops, and the measured discharge distance from the video substantiates the predicted range calculated with our model. *Trametes versicolor*, the species with the shortest discharge distance, is a small poroid fungus, and the fertile tissue is arranged into a layer of tightly packed tubes. The short discharge range is a great advantage to increase the opportunity that most spores can exit the tubes by reducing impaction on the opposing inner surface of tubes. *Polyporus squamosus* has comparatively wide and long tubes, 5 - 10 mm long compared with the tubes less than 2 mm long in *Trametes versicolor*. Therefore, longer discharge distance could decrease the probability of landing on the walls of the tubes during descent. *Cerrena unicolor* produce medium sized spores, and the discharge velocity and distance measurements are between *P. squamosus* and *T. versicolor*. Measurements and observations from the videos supported our hypothesis that there is a significant relationship between spore size and the tube (pore) size. Species having large tubes are likely to produce large spores, which affects the tube (pore) size.

The final size of Buller's drop and projectile size (spore size and the attached fluid after Buller's drop collapse) strongly influence spore discharge distance. The variation in spore size from the three species in this study produces an 80-fold range in Buller's drop size, which leads to a large energy difference when launching the spore. The aerodynamic drag force is resistant to the motion of the spore depending on the cross-sectional area of the moving object perpendicular to the flow. After it is propelled from the fertile tissue, the spore is confronted with decelerating drag force, which is proportional to the square of the spore radius. According to Newton's first law of motion, larger spores of higher mass, tend to maintain their original speed. Therefore, larger spores undergo less deceleration ( $a=F/m$ ) than small spores, resulting in longer flight distance. This velocity-dependent force also depends on the drag coefficient ( $C_d$ ), which is not a constant but varies with projectile speed, and object shape.  $C_d$  equals 0.4 for rough sphere ( $R_d=10^6$ ), and 0.1 for smooth sphere. A rough sphere could be regarded as a spore with protruding ridges in some species. Drag coefficient also changes in relation to the shape of the object. For example, a sphere has  $R_d = 0.47$ , while long cylinder has  $R_d = 0.82$ . The difference may explain the mismatch between the real measured distance and the calculated value based on our model.

#### **4.2 Development Rate of Buller's drop**

The development of Buller's drop occurs immediately after spore maturation. As the humidity in the Petri dish is simulated to natural conditions where spore are discharged, we regard the Buller's drop initiation and enlargement are approximately similar to the real process. We plotted the size of Buller's drop in *P. squamosus* to show how the volume of Buller's drop changes rapidly before the spore is released (Figure 4). From each video recording of Buller's drop formation in *P. squamosus*, we divided the video clips that focus on the development of Buller's drop to discharge into 10 phases, approximately 150 images, which represents the mean size of the Buller's drop at different phases (Figure 11). As shown in the graph, the enlargement rate of Buller's drop is constant. This indicates that the Buller's drop constantly imbibes water vapor from the surrounding air. The continuous enlargement of Buller's drop is of importance for the successful discharge of ballistospores. Several videos we captured showed how Buller's drop sometimes increased to exceed the size of the spore, and finally collapsed on to the spore

surface. This makes sense because if Buller's drop exceeds the normal size (usually diameter would not exceed the minor diameter of the spore), it would provide more energy to propel the spore over a longer distance, which may result in spore landing on the opposite of the pores or tubes. Therefore, the enlargement of Buller's drop allows the accumulation of the energy in the form of surface tension; meanwhile the final volume is confined by the spore volume to ensure enlargement is limited in an acceptable range.

### **4.3 Ballistospore Morphology**

Spore morphology in different agaricomycetes species were recorded using scanning electron microscopy (Figure 12). The basidiospores of *Polyporus squamosus* are the largest in the three species and also possess the longest hilar appendix where Buller's drop forms (Table 2).

*Polyporus badius* has much larger spores compared with *Trametes elegans*, but the hilar appendix length is relatively short, which is not able to support a large Buller's drop, and is therefore unable to launch the spore over a long distance. The pore size in this species is quite small, only 4-6/mm. *Trametes elegans* has small spores, but the length of the hilar appendix is proportionally large, which can produce larger Buller's drop to propel the spores to a long distance. This is accordant to the relatively low tube density of 1-2 /mm.

To summarize, the length of the hilar appendix correlates with the size of the spore to some extent, and further determines the size of Buller's drop. This morphological structure plays an important role in spore discharge mechanism by determining the angle and space that the drop forms to influence the energy providing device -- Buller's drop.

## **Chapter 5 Discussion**

### **5.1 Significance of Spore Morphology and the Size of the Buller's Drop**

Buller's drop size appears to affect discharge distance. The accepted model of the spore discharge mechanism suggests that the Buller's drop provides the energy for spore discharge. No matter what size the spore is, as long as it bears a large Buller's drop the moment before it discharges, it could be powered by the great amount of kinetic energy, thus allowing the spore travel a longer distance with sufficient "fuel." This case explains why small spores can travel a long distance. Therefore, it is reasonable to conclude that Buller's drop plays a very important role in the spore discharge distance.

Because the spore surface is hygroscopic, water vapor in the humid air will condense into Buller's drop. Hygroscopic absorption of water vapor continues until the Buller's drop makes contact with the expanding adaxial drop, and the movement of fluid drives spore discharge. The net energy released during the volume change from the Buller's drop to the final hemisphere fluid powers the launch; therefore the adaxial drop on the spore functions together with Buller's drop. The volume of the adaxial drop in some species changes significantly, but it is undistinguishable in others (Figure 13). This suggests that depending on habitat type and climate, humidity in the air may affect the accumulation of water on the concave side of the spore, and results in variation in the adaxial drop size, which may be another factor influencing the spore discharge mechanism.

The concentration of solutes in the Buller's drop is sufficient to bring about the condensation of water vapor from a saturated atmosphere and thus to cause the growth of Buller's drop at the measured rates. Successful basidiospore discharge can only occur when there is sufficient water vapor available to condense on the spore.

## 5.2 Evolutionary Trend between the Spore Size and the Pore or Tube Size.

The number of pores per mm does not always indicate the size of the pores, and in some species, the walls, or dissepiments, are so thick that the real size of the pores with density of 4 - 5 pores per mm may be the same pore size as ones with 7 - 10 pores per mm. This was unavoidable, because the taxonomic description did not include measurement of wall thickness.

Airborne basidiospores function as the reproductive units, and larger spores have a greater chance to survive. Variations in spore size and shape are determined by many parameters. Natural selection favors larger offspring, which represent the higher fitness in the environment; however, higher fitness and higher survival rate are at the cost of more nutrient and energy input for the parents (Stearns, 1992). The spore size varies with the basidiocarp size, as larger basidiocarps produce larger spores (Kausrud, 2008). Meerts (1999) reported previously the similar trend occurring in agarics. The similar relationship between spore size and the fruiting body size may represent a general pattern in fungal evolution. Though larger sized polypores produce large spores, the relationship between size of the basidiocarp and the tube size remains untested in fungi. Spores are produced on the basidium, the size of which is proportional to the size of spores. The larger the spore, the fewer basidia are produced per area of hymenium. In order to produce a large number of spores, species producing large spores tend to produce a large basidiocarp, or long tubes. It is obviously that longer tubes may present a disadvantage for the spore liberation; neither the humidity nor temperature in the deep tube may favor the spore falling course after discharge. Therefore, species with small spores may have a small and thin basidiocarp with tightly compacted pores, e.g., *Trametes versicolor* (fertile layer around 0.5 -1 mm thick); large spore producing polypores may have tubes as long as 10 mm.

The dominant way that fungi reproduce is by spore dispersal, and spore morphology plays an important role in this process. However, the spore size and shape have not received enough attention. The research around the relationship between basidiospore size, shape and life history characteristics (Kausrud, 2008) revealed that variance of basidiocarp size and nutritional mode are accounting for variation in spore size and shape. They came to a conclusion that species characterized by large basidiocarps tend to produce larger spores, and the shape of larger spores

tend to be more spherical. Potentially, many aerodynamic properties are under the influence of the spore shape. Spherical spores gain higher speeds more easily than narrow elongated spores in the air, though narrow spores float better through the air after their liberation (Deacon, 1997). The polypores are characterized by poroid basidiocarps, however the size of pores range widely. It is necessary to study whether there is a pattern between the sizes of fruiting bodies and the fertile tubes they produce.

The path of discharged spores must be confined to a limited distance from the inner surface of tubes in poroid fruiting bodies. For the fungi with exposed hymenophores, spores are discharged directly into the free air. That may explain why ballistospores in those species could be launched a longer distance.

Initially, we did attempt to collect as much as poroid agaricomycetes including the boletes, but it was found that hymenia in some species were very soft and sensitive to desiccation and intense light, meanwhile it was not possible to collect enough species during the dry season. The capture of the sequence is time consuming and fresh mushrooms could only be preserved for several days. Therefore, we were unable to collect useful data from these species. In the future, data involved in spore discharge process from other order in poroid basidiomycetes are still needed to solidify our hypotheses. Meanwhile, the spores were recorded to deposit along the hymenium within certain range after discharge, rather than being launched in to the center of the tube, therefore the spore discharge distance is not confined to the tube size (Figure 14). In this case, species with wider tubes may not explain that larger spores tend to be produced in larger tubes.

In conclusion, we think that the analysis of high speed video camera sequence collected from the three species presented in this thesis provides an important conceptual focus for further and more detailed analysis of the evolution of poroid agaricomycete fungi. The key objective of this study was to test whether or not there is a relationship between spore size and tube size, and to explore how this might be linked to the spore discharge mechanism. The data obtained from the three species of poroid agaricomycetes will aid future exploration of the significance of the discharge mechanism in affecting spore size and discharge distance, and will facilitate further studies into the spore discharge process.

## References

Alexopoulos, C. J., Mims, C. W., and Blackwell, M. 1996. *Introductory Mycology*. 4<sup>th</sup> Edition. John Wiley & Sons, INC.

Barron, G. 1999. *Mushrooms of northeast North America*. Lone Pine, Canada. Pp: 336.

Bessette, A. E., Bessette, A. R., and Fischer, D. W. 1997. *Mushrooms of Northeastern North America*. Syracuse University Press.

Bessette, A. E., Roody, W. C., and Resette, A. R. 2000. *North American Boletes*. Syracuse University Press.

Binder, M., and Hibbett, D. S. 2002. Higher - level phylogenetic relationships of homobasidiomycetes (mushroom-forming fungi) inferred from four rDNA regions. *Molecular Phylogenetics and Evolution* 22: 76-90.

Bozzola, J. J., and Russell, L. D. 1998. *Electron Microscopy: Principles and Techniques for Biologists*. 2<sup>th</sup> Edition. Sudbury, Massachusetts, Jones and Bartlett Publishers, Inc.

Buller, A. H. R. 1909. *Researches on Fungi*. Longmans Green, London.

Corner, E. J. D. 1948. Studies in the basidium I. The ampoule effect with a note on nomenclature. *New Phytologist* 47: 22-51.

Deacon, J. W. 1997. *Modern Mycology*. 3<sup>rd</sup> Edition. Blackwell Science Ltd.

Deering, R., Dong, F., Rambo, D., and Money, N. P. 2001. Airflow patterns around mushrooms and their relationship to spore dispersal. *Mycologia* 93: 732-736.

Donk, M. A. 1964. A conspectus of the families of the Aphylophorales. *Persoonia* 3: 199-324.

Kher, K., Greening, J. P., Hatton, J. P., Novak Frazer, L., and Moore, D., 1992. Kinetics and mechanics of stem gravitropism in *Coprinus cinereus*. *Mycological research* 96: 817-824.

Gilbertson, R. L., and Ryvarden, L. 1986. *North American Polypores*. Volume 1. Fungiflora A/S Oslo, Norway.

Gilbertson, R. L., and Ryvarden, L. 1987. *North American Polypores*. Volume 2. Fungiflora A/S Oslo, Norway.

Gregory, P. H. 1957. Electrostatic charges on spores of fungi in air. *Nature* 180: 330.

Hallenberg, N., and Kuffer, N. 2008. Long-distance spore dispersal in wood-inhabiting Basidiomycetes. *Nordic Journal of Botany* 21: 431-436.

Hawksworth, D. L. 1991. The fungal dimension of biodiversity: magnitude, significance, and conservation. *Mycological Research* 95: 641-655.

Hibbett, D. S., M. Binder, J. F. Bischoff, M. Blackwell, P. F. Cannon, O. E. Eriksson, S. Huhndorf, T. James, P. M. Kirk, R. Lücking, T. Lumbsch, F. Lutzoni, P. B. Matheny, D. J. McLaughlin, M. J. Powell, S. Redhead, C. L. Schoch, J. W. Spatafora, J. A. Stalpers, R. Vilgalys, M. C. Aime, A. Aptroot, R. Bauer, D. Begerow, G. L. Benny, L. A. Castlebury, P. W. Crous, Y.-C. Dai, W. Gams, D. M. Geiser, G. W. Griffith, C. Gueidan, D. L. Hawksworth, G. Hestmark, K. Hosaka, R. A. Humber, K. Hyde, J. E. Ironside, U. Kõljalg, C. P. Kurtzman, K.-H. Larsson, R. Lichtwardt, J. Longcore, J. Miądlikowska, A. Miller, J.-M. Moncalvo, S. Mozley-Standridge, F. Oberwinkler, E. Parmasto, V. Reeb, J. D. Rogers, C. Roux, L. Ryvarden, J. P. Sampaio, A. Schüßler, J. Sugiyama, R. G. Thorn, L. Tibell, W. A. Untereiner, C. Walker, Z. Wang, A. Weir, M. Weiß, M. M. White, K. Winka, Y.-J. Yao, and N. Zhang. 2007. A higher-level phylogenetic classification of the Fungi. *Mycological Research* 111: 509-547.

Hibbett, D. S. 2006. A phylogenetic overview of the Agaricomycotina. *Mycologia* 98: 917-925.

- Hibbett, D. S., and Donoghue, M. J. 1995. Progress toward a phylogenetic classification of the Polyporaceae through parsimony analysis of mitochondrial ribosomal DNA sequences. *Canadian Journal of Botany* 73: 85-861.
- Husher, J., Cesarov, S., Davis, C. M., Fletcher, T. S., Muthia, K., Richey, L., Sparks, R., Turpin, L. A., and Money, N. P. 1999. Evaporative cooling of mushrooms. *Mycologia* 91: 351-352.
- Ingold, C. T. 1939. Spore Discharge in Land Plants. Clarendon Press, Oxford.
- Ingold, C. T. 1992. The basidium: a spore gun of precise range. *Mycologist* 6: 111-113.
- Ingold, C. T. 1998. Ballistosporic basidia. *The Mycologist* 12: 50-52.
- Kauserud, H., Colman, J. E., and Ryvarden, L. 2008. Relationship between basidiospore size, shape and life history characteristics: a comparison of polypores. *Fungal Ecology* 1: 19 -23.
- Kirk, P. M., Cannon, P. F., David, J. C., and Stalpers, J. 2001. *Ainsworth and Bisby's Dictionary of the Fungi*. 9<sup>th</sup> Edition. CAB International, Wallingford, UK.
- Kramer, C. L. 1982. Production, release and dispersal of basidiospores. In: *Decomposer Basidiomycetes: their biology and ecology*. Cambridge University Press, Cambridge, UK. Pp. 33-49.
- Larsen, M., and Lombard, F. F. 1988. The status of *Meripilus giganteus* (Aphyllophorales, Polyporaceae) in North America. *Mycologia* 80: 612-21.
- Lincoff, G. H. 1981. *The Audubon Society field guide to North American mushrooms*. New York: Knopf. See also Lincoff, G. H. (1985) "A key to gilled mushrooms in the Audubon field guide."
- McLaughlin, D. M., Beckett, A., and Yoon, K. S. 1985. Ultrastructure and evolution of ballistosporic basidiospores. *Botanical Journal of the Linnean Society* 91: 253-271.

- Meert, P. 1999. The evolution of spore size in Agarics: do big mushrooms have big spores? *Journal of Evolutionary Biology* 12: 161-165.
- Mims, C. W., and Richardson, E. A. 2005. Ultrastructure of sporodochium and conidium development in the anamorphic fungus *Epicoccum nigrum*. *Canadian Journal of Botany* 83: 1354-1363.
- Money, N. P. 1998. More g's than the space shuttle: Ballistospore discharge *Mycologia* 90: 547-558.
- Money, N. P., and Fischer, M. 2008. Biomechanics of spore discharge in phytopathogens. In: Deising, H. eds. *The Mycota, Volume V, Plant Relationships*, 2<sup>nd</sup> Edition. Springer Verlag, New York Press.
- Monzer, J., Haindl, E., Kern, V., and Dressel, K. 1994. Gravitropism of the basidiomycete *Flammulina velutipes*: morphological and physiological aspects of the graviresponse. *Experimental Mycology* 18: 7-19.
- Moore-Landecker, E. 1996. *Fundamentals of the Fungi*. 4<sup>th</sup> Edition. Prentice Hall, Upper Saddle River, New Jersey.
- Olive, L. S. 1964. Spore discharge mechanism in basidiomycetes. *Science* 23: 542-543.
- Phillips, R. 1991. *Mushrooms of North America*. Boston: Little, Brown and Company. Pp. 319.
- Phillips, R. 2006. *Roger's Mushrooms*. Retrieved from the World Wide Web: <http://www.rogersmushrooms.com/>
- Pringle, A., Patek, S. N., Fischer, M., Stolze, J., and Money, N. P. 2005. The captured launch of a ballistospore. *Mycologia* 97: 866-871.

Ross, I. K. 1979. *Biology of the Fungi: their development, regulation and association*. McGraw-Hill Series, New York.

Savile, D. B. O. 1965. Spore discharge in basidiomycetes: A unified Theory. *Science* 8: 165-166.

Stearns, S. C. 1992. *The Evolution of Life Histories*. Oxford University Press, Oxford, England.

Stolze-Rybczynski, J. L., Cui, Y., Stevens, M. H. H., Davis, D. J., Fischer, M. W. F., and Money, N. P. 2009. Adaptation of spore Discharge Mechanism in the Basidiomycota. *PLoS ONE* 4: e4163.

Swift, M. J., Frankland, J. C., and Hedger, J. N, eds. 1982. *Decomposer Basidiomycetes: Their Biology and Ecology*, Cambridge University Press. Pp. 307-337.

Thiers, H. D. 1984. The secotioid syndrome. *Mycologia* 76: 1-8.

Turner J., and Webster J. 1991. Mass and Momentum-Transfer on the Small-Scale-How Do Mushrooms shed Their Spores. *Chemical Engineering Science*. 46: 1145-1149.

Van Niel, C.B., Garner, G. E., and Cohen, A. L. 1972. On the mechanism of Ballistospore Discharge. *Archives of Microbiology* 84: 129-140.

Webster, J. 1952. Spore projection in the hyphomycete *Nigrospora tphaaerica*. *New Phytol* 52: 229-235.

Webster, J. 1980. *Introduction to Fungi*. 2<sup>nd</sup> Edition. Cambridge University Press.

Webster, J., and Chen, C. Y. 1990. Ballistospore discharge. *Transactions of the Mycological Society of Japan* 31: 301-31.

Webster, J., Davey, R. A., Smirnoff, N., Fricke, W., Hinde, P., Tomos, D., and Turner, J. C. R. 1995. Mannitol and Hexoses are components of Buller's Drop. *Mycological Research* 99: 833-838.

Webster, J., Davey, R. A., and Turner, J. C. R. 1989. Vapor as the source of water in Buller's drop. *Mycological Research* 93: 297-302.

Webster, J., Proctor, M. C. R., Davey, R. A., and Duller, G. A. 1988. Measurement of the electrical charge on some basidiospores and an assessment of two possible mechanisms of ballistospore propulsion. *Transactions of the British Mycological Society* 91: 193-203.

**Table 1.** Ballistospore discharge in three polypores.

Polyporales Species*	Initial velocity, m/s measured range, mean $\pm$ s.e.m	Measured discharge distance (mm)	Calculated discharge distance (mm)	Spore size ( $\mu$ m)	Radius of Buller's drop ( $\mu$ m)	Tube size (mm) pores/mm
<i>Polyporus squamosus</i>	0.45 - 0.68 0.58 $\pm$ 0.08 (8)	0.075 - 0.15 0.13 $\pm$ 0.02 (6)	0.14 (6)	14.0 x 5.4 (31)	2.6 (16)	1-3 x 0.5-1.5
<i>Cerrena unicolor</i>	0.54 - 0.70 0.62 $\pm$ 0.04 (2)	0.037 - 0.066 0.041 $\pm$ 0.03 (2)	0.045 (2)	4.5 x 2.7 (3)	1.5 (1)	0.18 2-3
<i>Trametes versicolor</i>	0.35 - 0.70 0.68 $\pm$ 0.07 (6)	0.028 - 0.048 0.03 $\pm$ 0.02 (6)	0.018 (6)	5.4 x 1.5 (31)	0.6 (6)	0.083 4-5

\* Data also applied in the paper from Stolze-Rybczynski, 2009.

Sample sizes in parenthesis.

Calculated discharge distance using mean values for spore dimensions, drop size, and velocity.

**Table 2.** Sizes of spores and hilar appendix in three polypores.

Polyporales species	Width and length of basidiospores ( $\mu$ m)	Length of hilar appendix ( $\mu$ m)	Tube size ( $\mu$ m) pores/mm
<i>Polyporus squamosus</i>	9.55 $\pm$ 0.09 x 3.62 $\pm$ 0.10	0.62 $\pm$ 0.03	1-3 x 0.5-1.5
<i>Polyporus badius</i>	6.01 $\pm$ 0.09 x 3.16 $\pm$ 0.08	0.27 $\pm$ 0.03	4-6
<i>Trametes elegans</i>	4.31 $\pm$ 0.06 x 1.92 $\pm$ 0.08	0.30 $\pm$ 0.03	1-2
<i>Ganoderma applanatum</i>	6.82 $\pm$ 0.04 x 4.90 $\pm$ 0.03	0.23 $\pm$ 0.05	4-6
<i>Trametes versicolor</i>	5.22 $\pm$ 0.09 x 1.89 $\pm$ 0.07	0.43 $\pm$ 0.05	4-6

**Figure 1.** Diverse hymenophore structures in (a) *Ganoderma applanatum*, (b) *Pycnoporus cinnabarinus*, (c) *Trametes hirsuta*, (d) *Laetiporus sulphae*, (e) *Trametes versicolor*, and (f) *Ganoderma lucidum*. Bar = 1 mm.

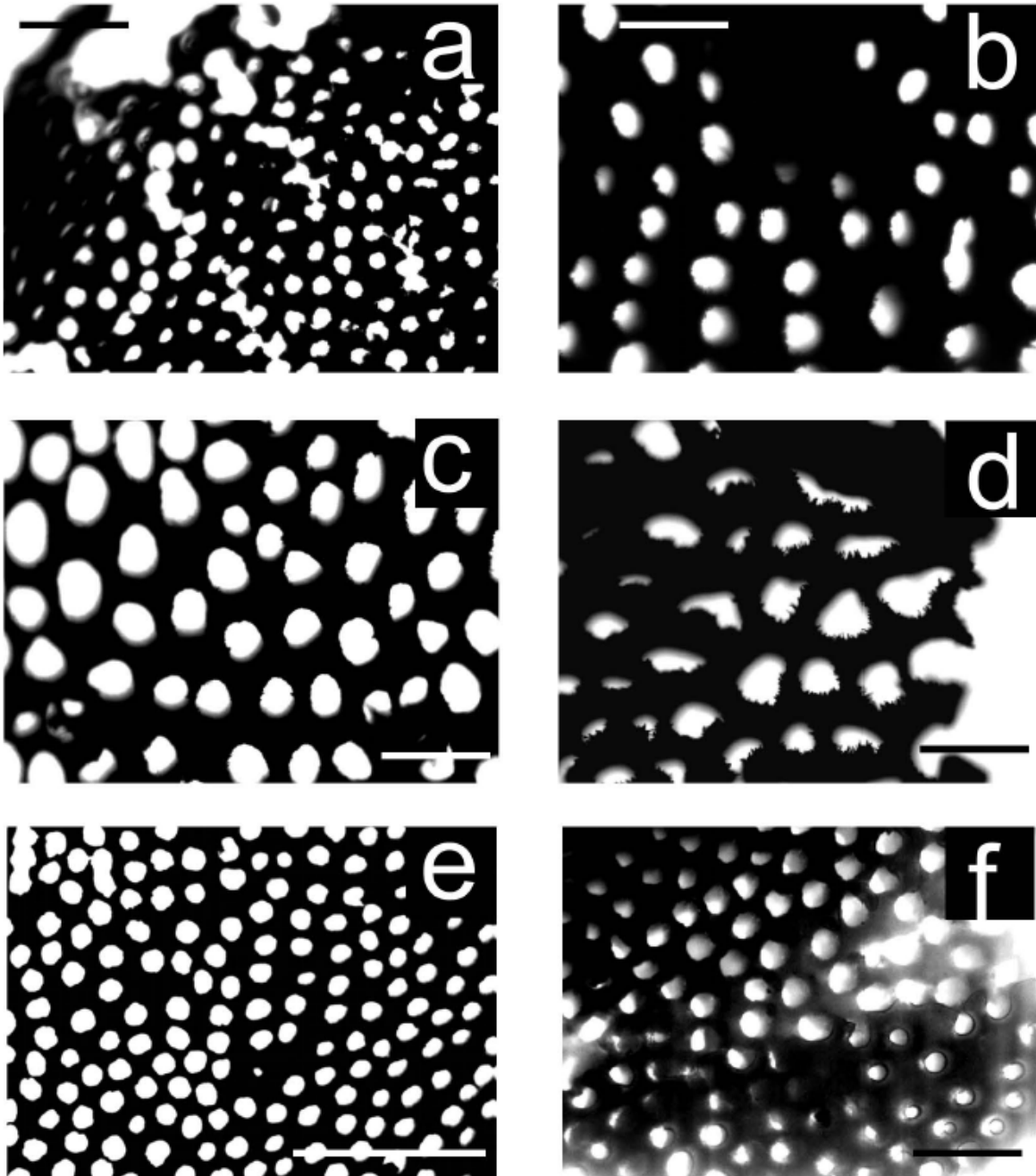


**Figure 2.** Basidia bearing ballistospores in (a) *Polyporus squamosus*, and (b) *Polyporus badius*.  
Bar = 20  $\mu$ m.

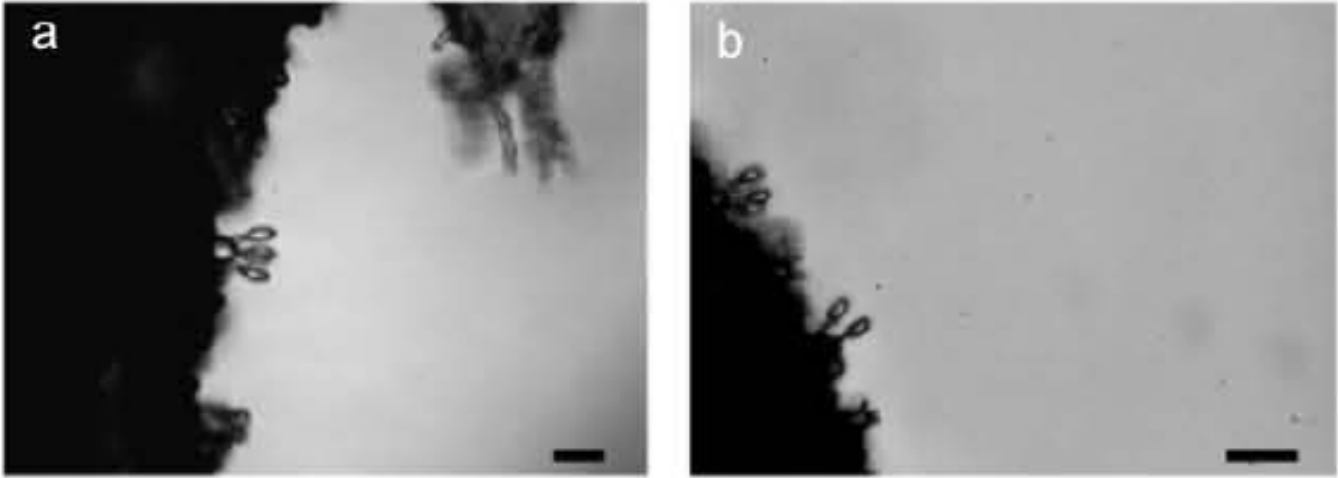


**Figure 3.** Morphology of six polypore species. (a) *Polyporus squamosus*; (b) *Trametes versicolor*; (c) *Polyporus badius*; (d) *Trametes elegans*; (e) *Cerrena unicolor*; (f) *Ganoderma applanatum*.

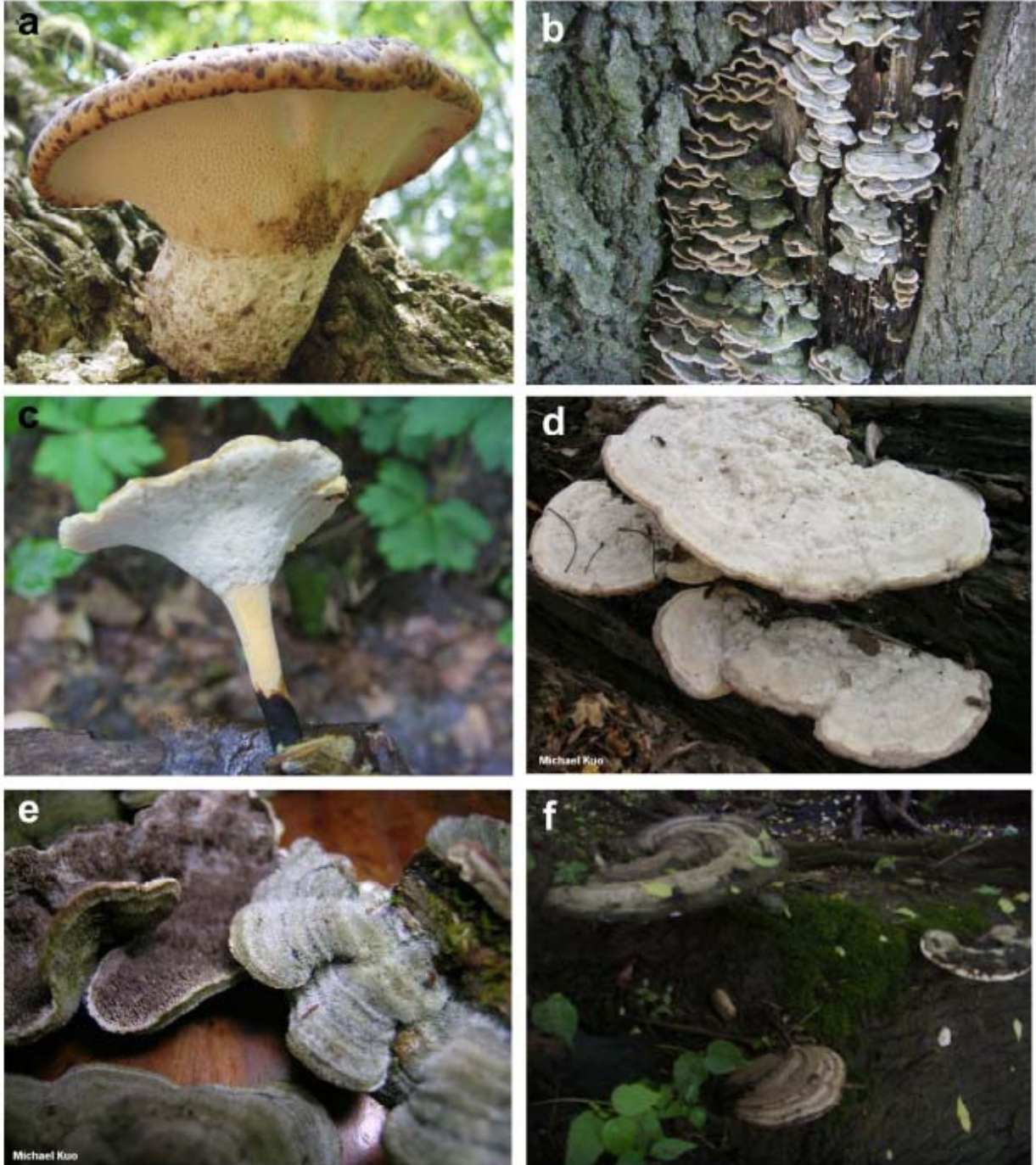


**Figure 4.** Spore discharge process in *Polyporus squamosus*. Buller's drop initiates at the base of the basidiospore, and enlarges by accumulating the water vapor from the environment.

Bar = 40  $\mu\text{m}$ .

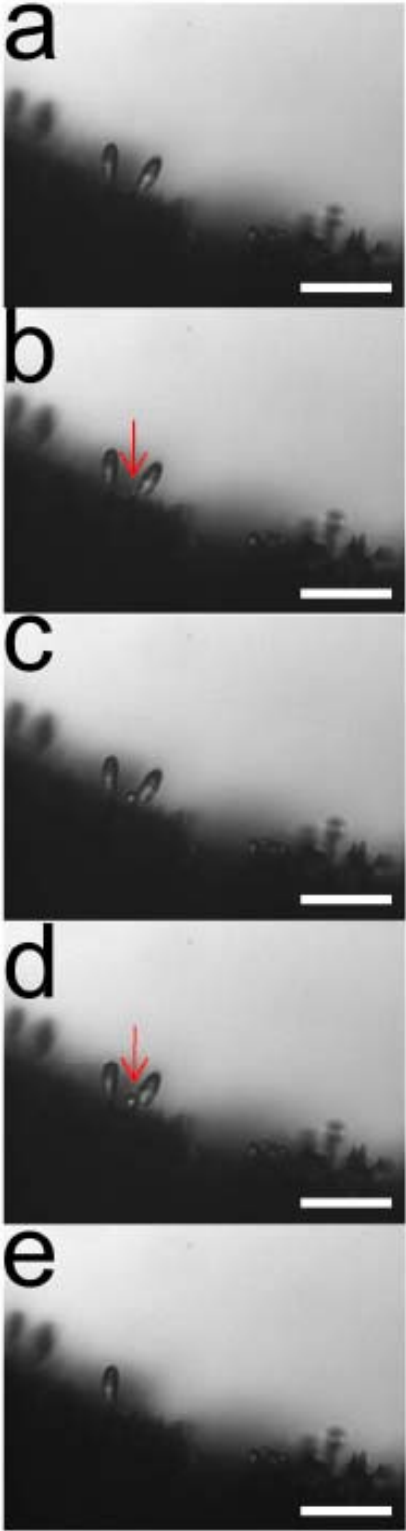


**Figure 5.** The process of ballistospores fungi shedding spores from the sterigma. (a) the structure of a basidiospore supported by sterigma. The hilar appendix characterizes the bilaterally symmetric spores, which link the spore to the sterigma. Emerge of the Buller's drop at the point of contact of the spore and the sterigma on the concave side of the spore and gradually enlarges until it reaches a size of almost half that of the spore (b-e). The process depicts the surface tension catapult, driven by the collapse of Buller's drop and the adaxial drop (Stolze-Rybczynski *et al.*, 2009).

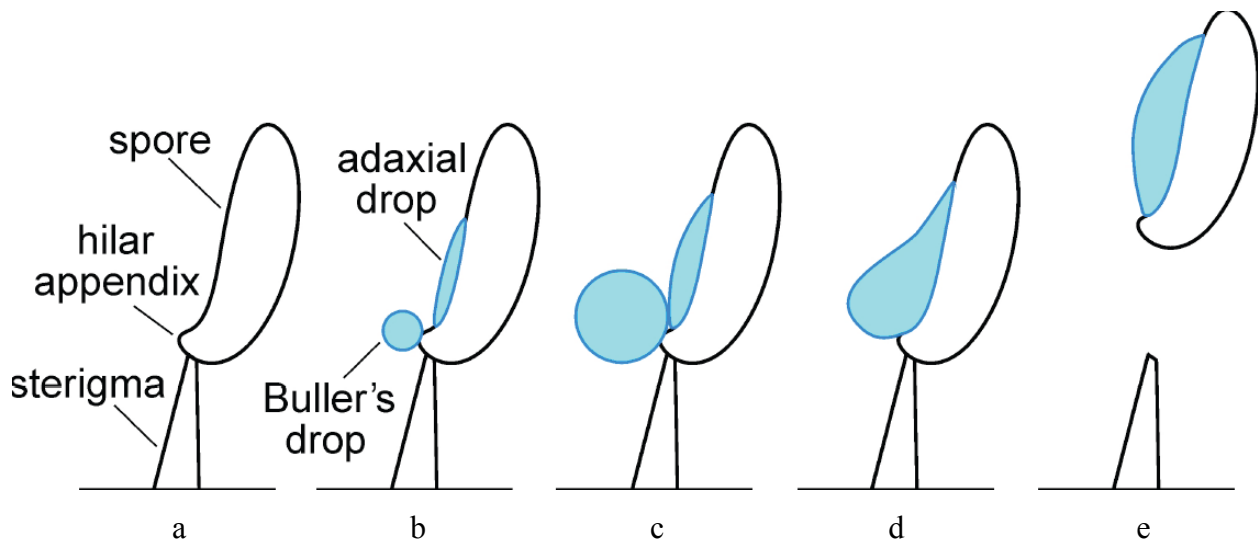
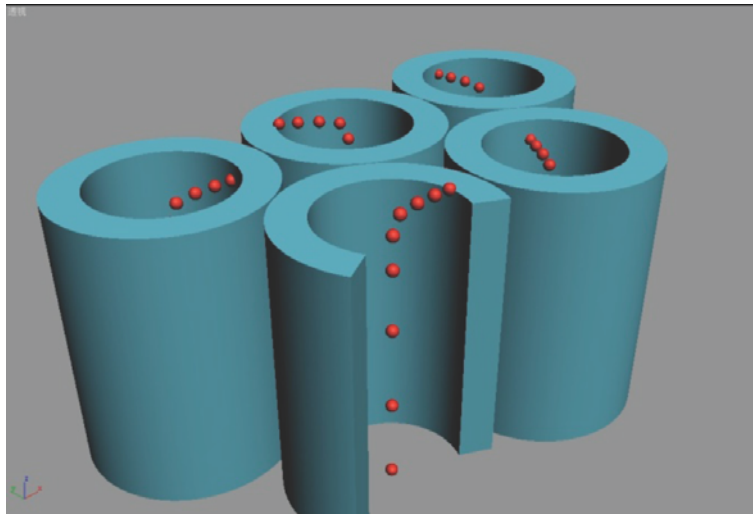
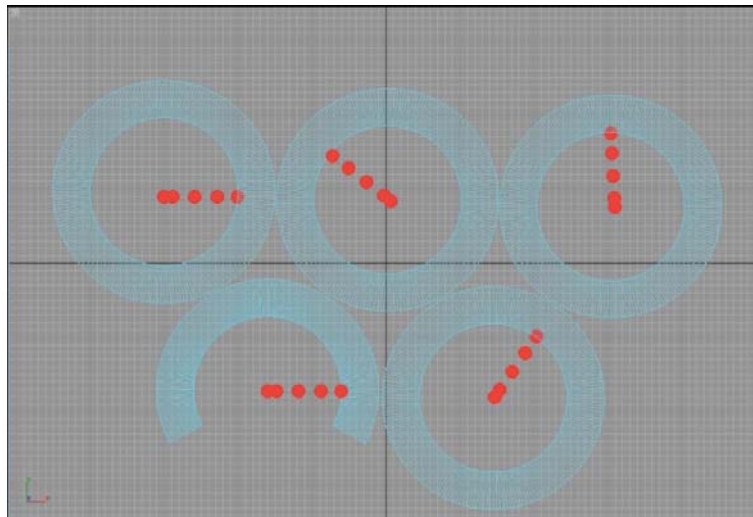


**Figure 6.** Pathway of spores after discharge from the inner surface of tubes in a poroid fruiting body, shown in 3-D and 2-D plane images, respectively. The successive red dots represent the pathway of a discharged basidiospore released from one spot on the hymenium of a tube on side and planform views. Usually, the maximum horizontal distance the spore could reach is about the radius of the hymenium tube where the spore launched. Then the overwhelming air viscosity stops the spore from going further, and under gravity, spores fall through the tubes vertically.

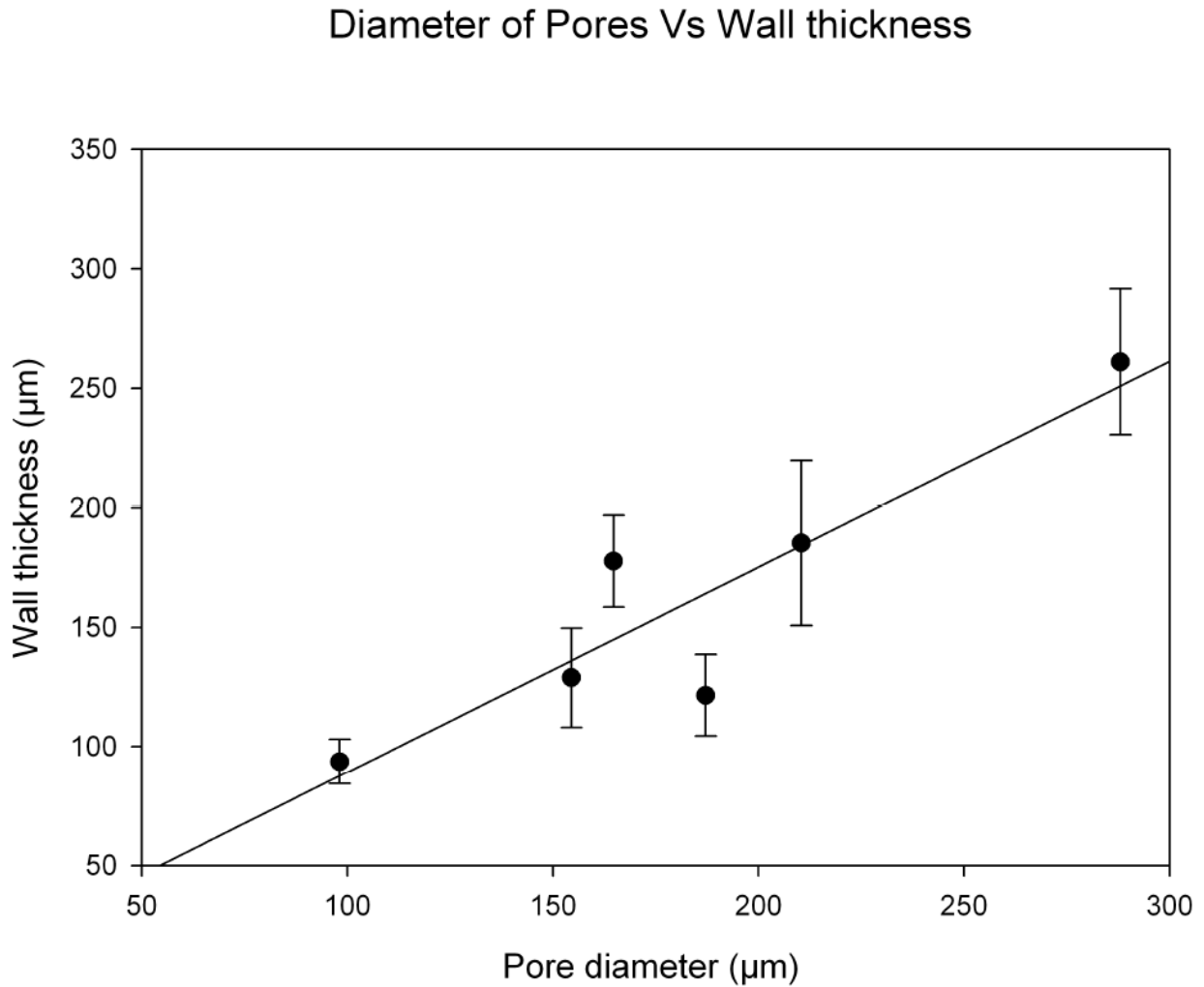


a

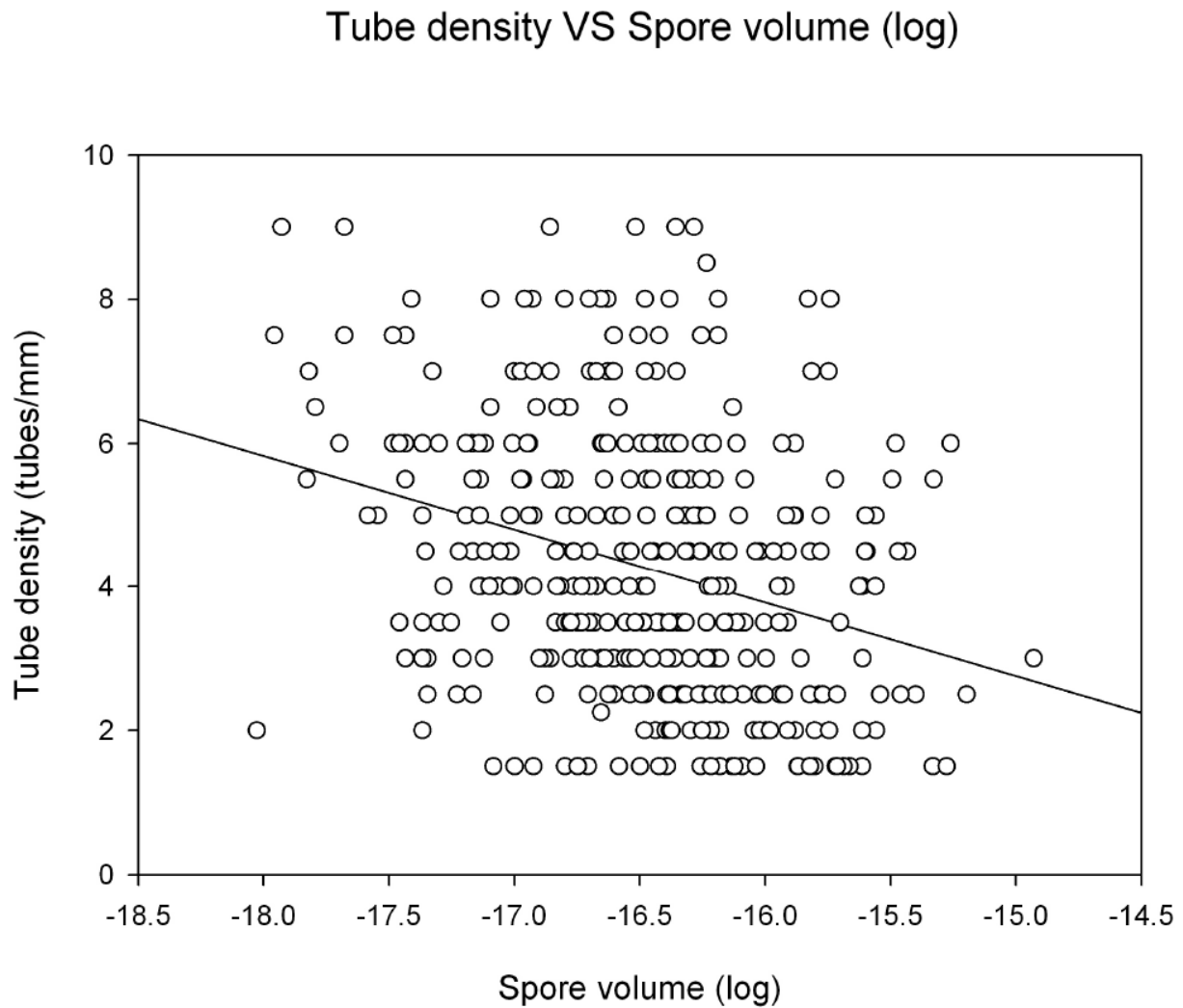


b

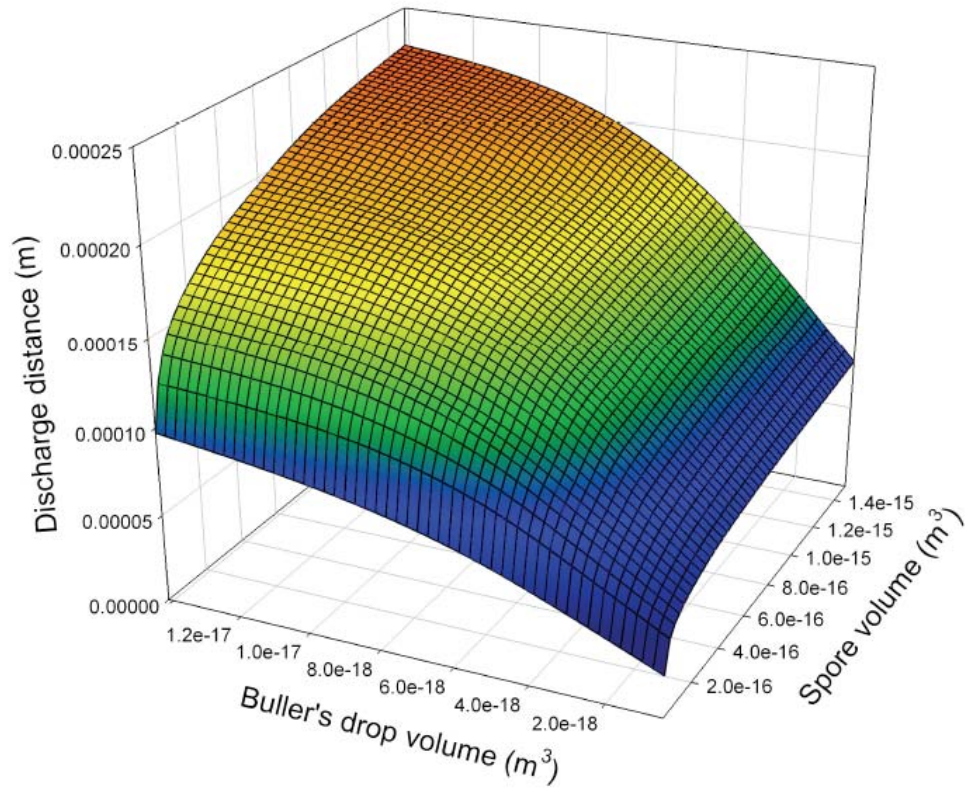
**Figure 7.** Relationship between the pore diameter and the wall thickness. The thickness of the tissue between the pores varies among different species. Six species will poroid hymenophore were used to test the relationship between the wall thickness and the pore diameter. CI: 95%,  $r^2$ : 0.83.



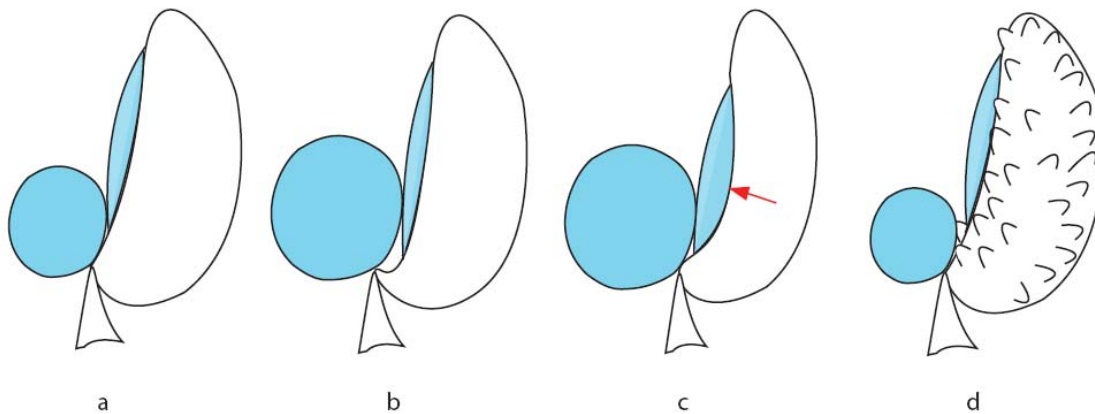
**Figure 8.** Relationship between spore volume and tube size plotted in logarithm based on 237 species of polypores with poroid fruiting bodies (Stolze-Rybczynski, 2009). The ordinary least-squares (OLS) Regression shows larger spores are related with larger tubes, and vice versa. However, the data are so scattered in the graph, which indicates that spore volume has faint relationship with tube radius, unable to explain the expected positive correlation between average tube radius and spore volume.



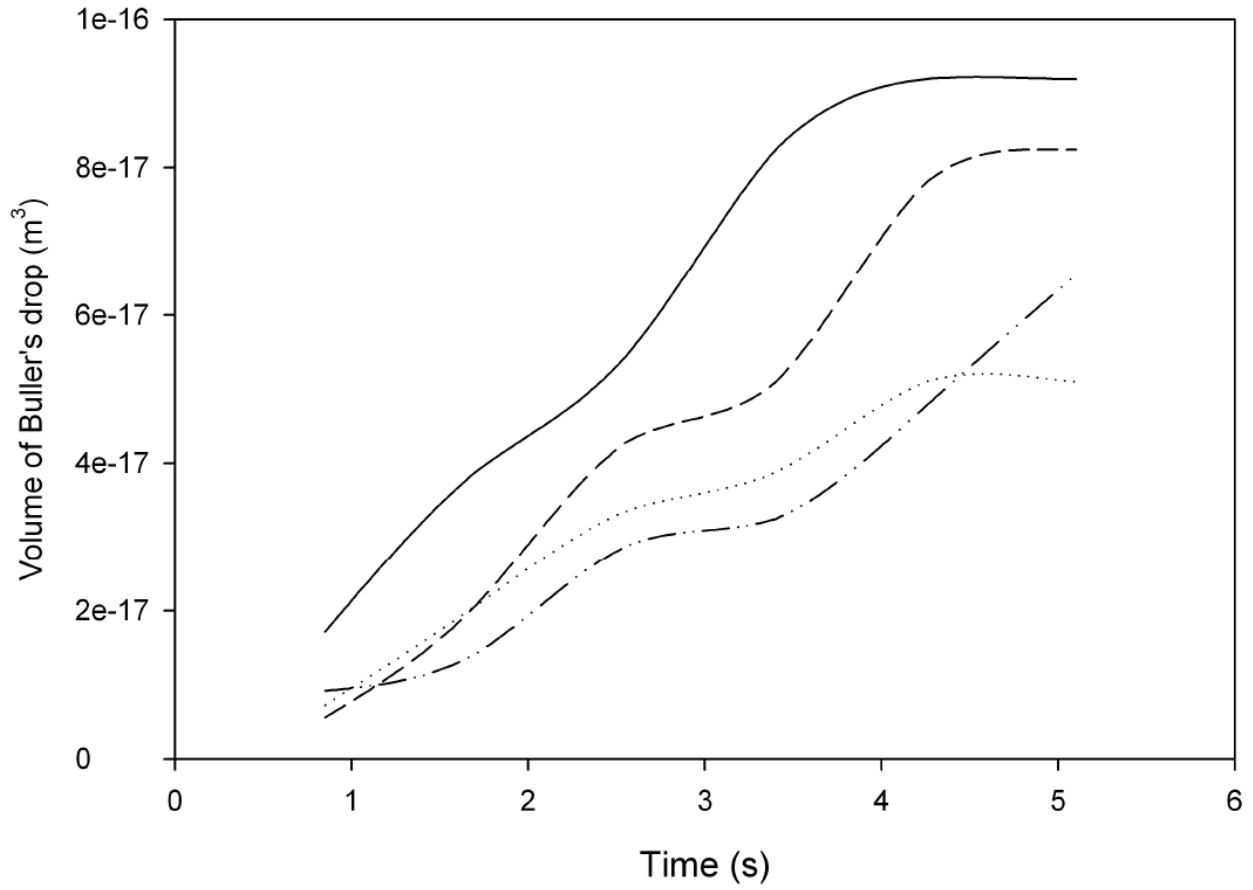
**Figure 9.** Graph showing the relationship between spore volume, Buller's drop volume, and discharge distance among 61 species of polypore. Larger spores bearing different volumes of Buller's drop seems to have a wide range of the spore discharge distance compared with small spores.



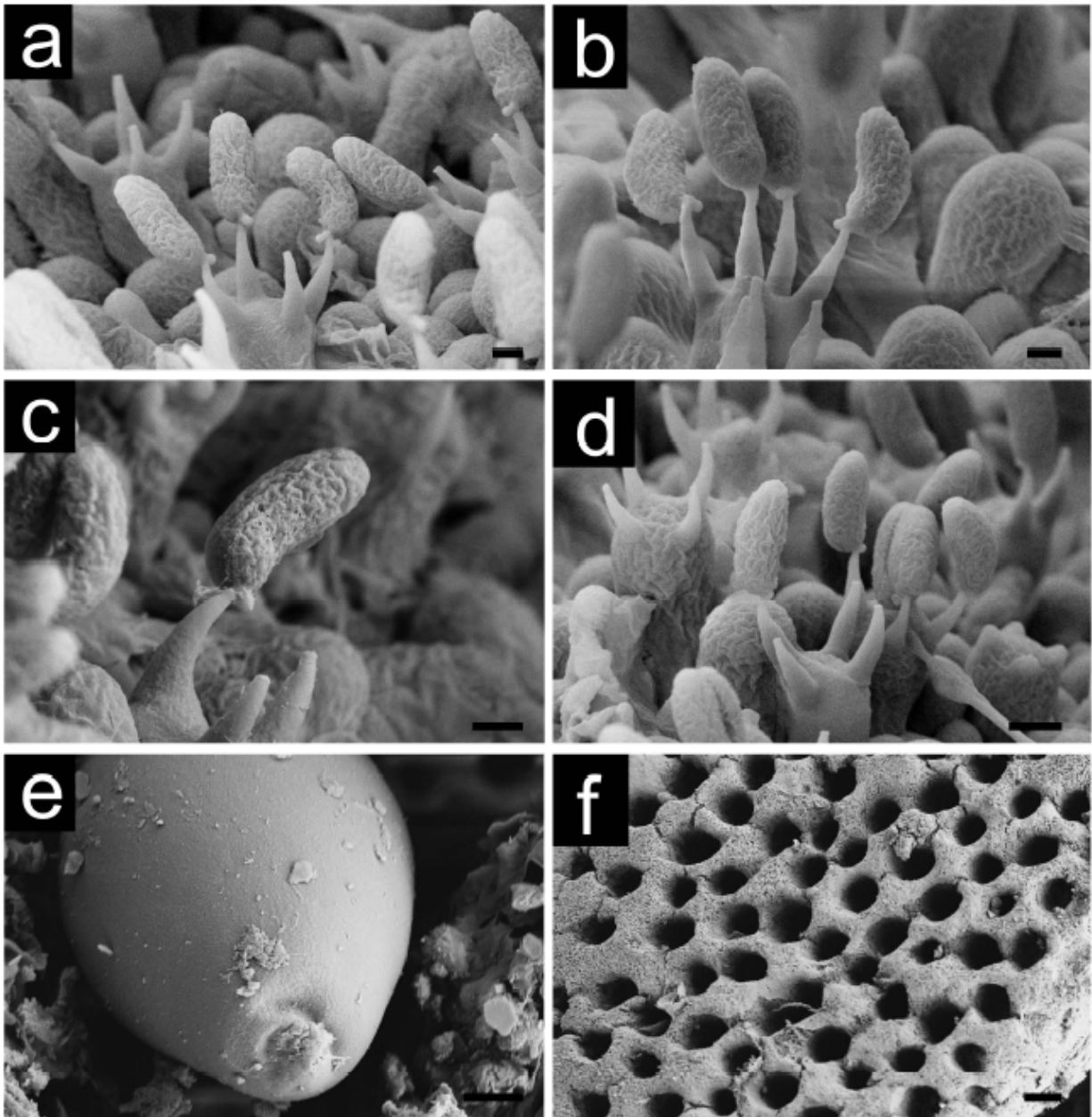
**Figure 10.** Effects of spore morphology on the development of Buller's drop. The spore size is the same from (a) to (d). (a) Buller's drop reaches its largest size immediately before it collapses with the adaxial drop. (b) If the same sized spore has a longer hilar appendix, the final size of Buller's drop would be larger than that in a, which means large potential force to launch the spore. (c) Suprihila disc characterizes some basidiospores. The concave area provides more space for Buller's drop enlargement. (d) Basidiospores decorated with ridges or spikes are presented in some species. In this case, the final size of Buller's drop may be very small before it contacts with the fluid film on the spore surface.



**Figure 11.** Development rate of the Buller's drop in *Polyporus squamosus*. S.1-S.4 represent four selected video sequences recording the Buller's drop enlargement before spore discharge.



**Figure 12.** Scanning electron micrographs of spores and basidia in (a-d) *Trametes versicolor*; (e-f) *Ganoderma applanatum*; (g-h) *Trametes elegans*; (i-j) *Polyporus badius*; (k-n), *Polyporus squamosus*. Spores shrink slightly during preparation. Bar = 1  $\mu\text{m}$  (a-c, k, and l), 2  $\mu\text{m}$  (d, i, j, and m-n), 4  $\mu\text{m}$  (e), 100  $\mu\text{m}$  (f).



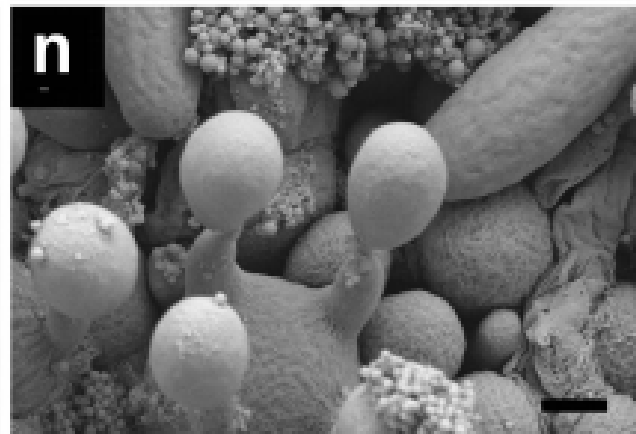
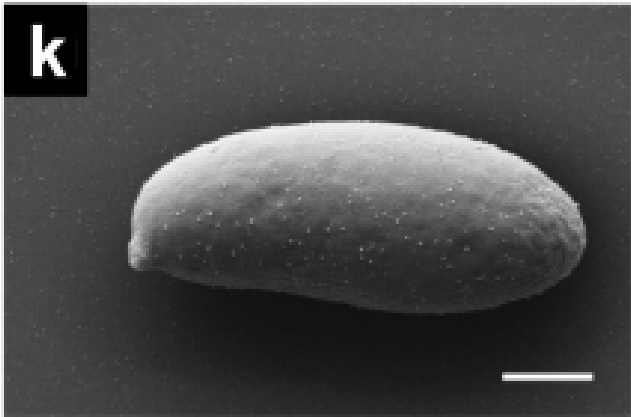
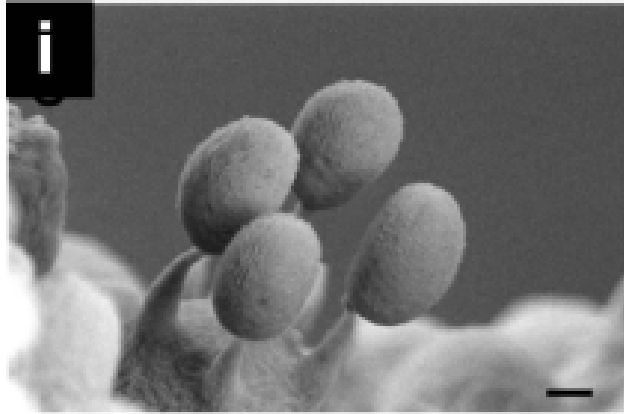
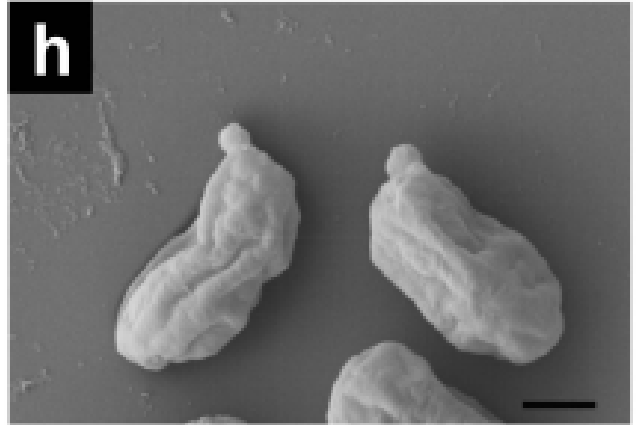


**Figure 13.** Successive images showing spore discharge in *Trametes versicolor*. As shown in the images, the adaxial drop emerging on the adjacent side of the spore is growing before the spore is discharged. Bar = 10μm. Camera speed = 24 fps.

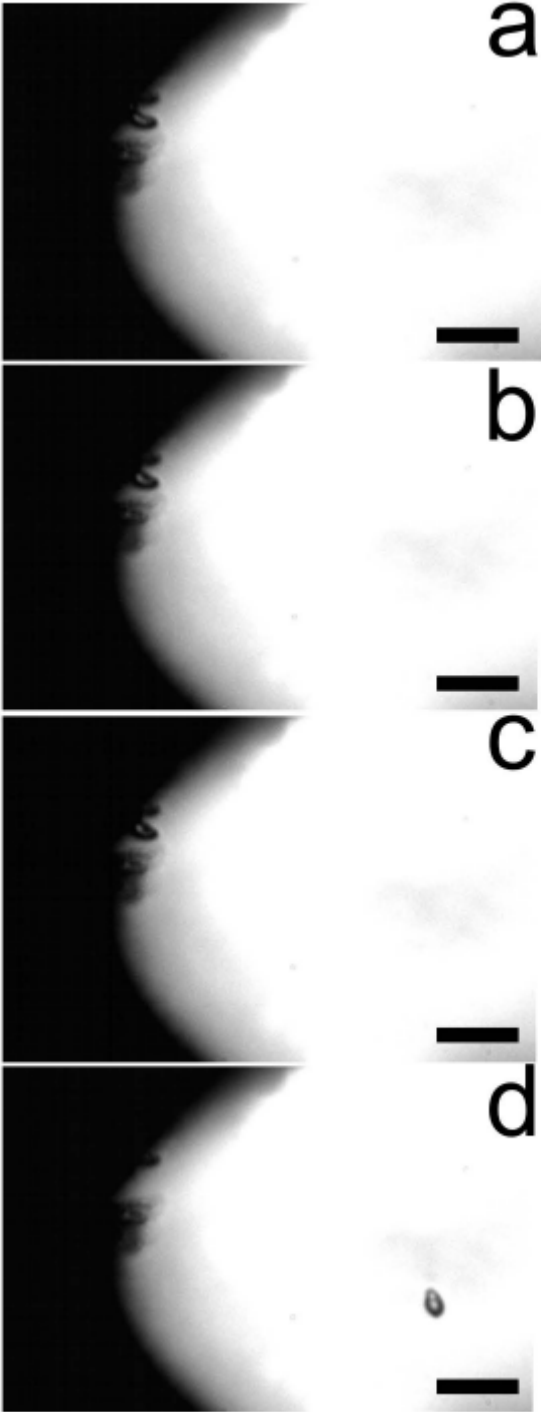
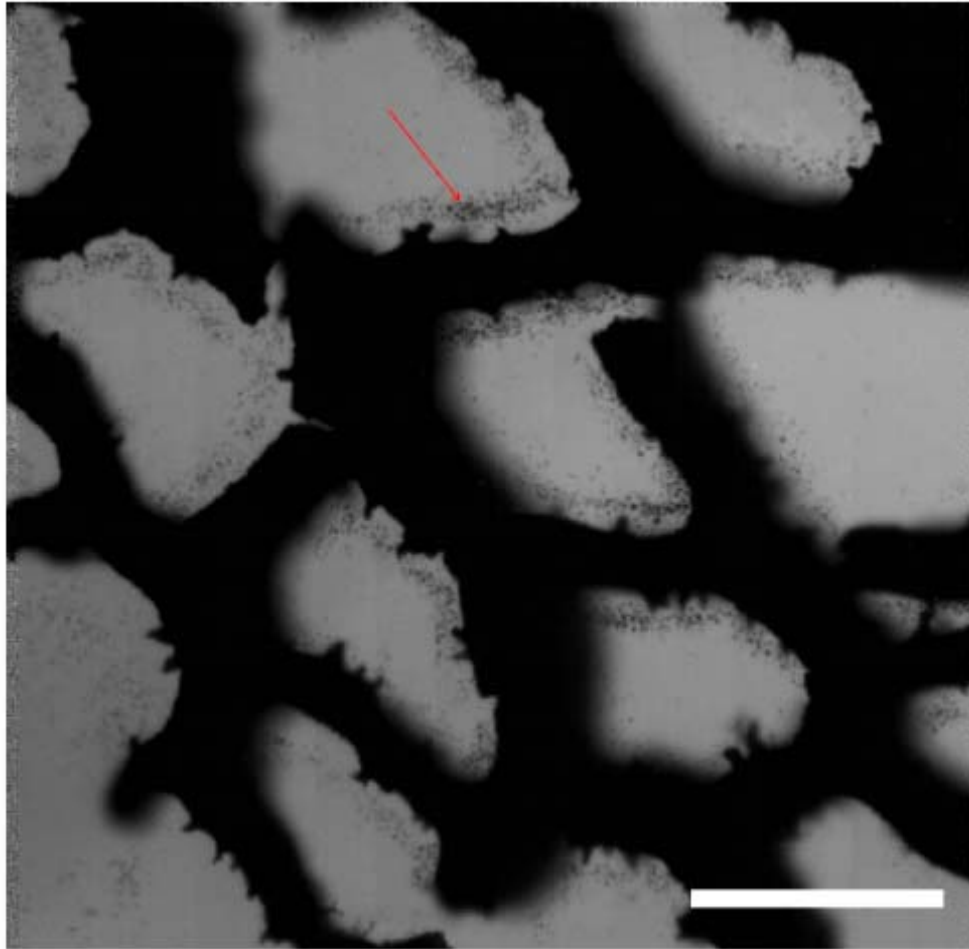
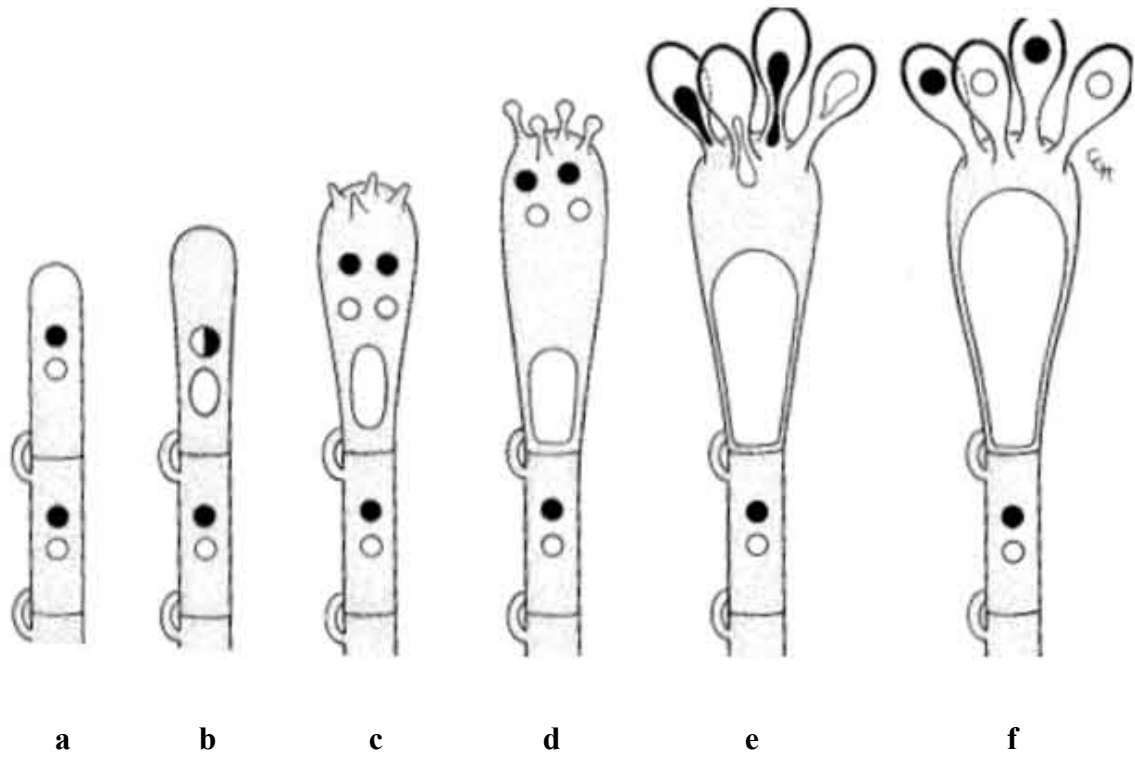


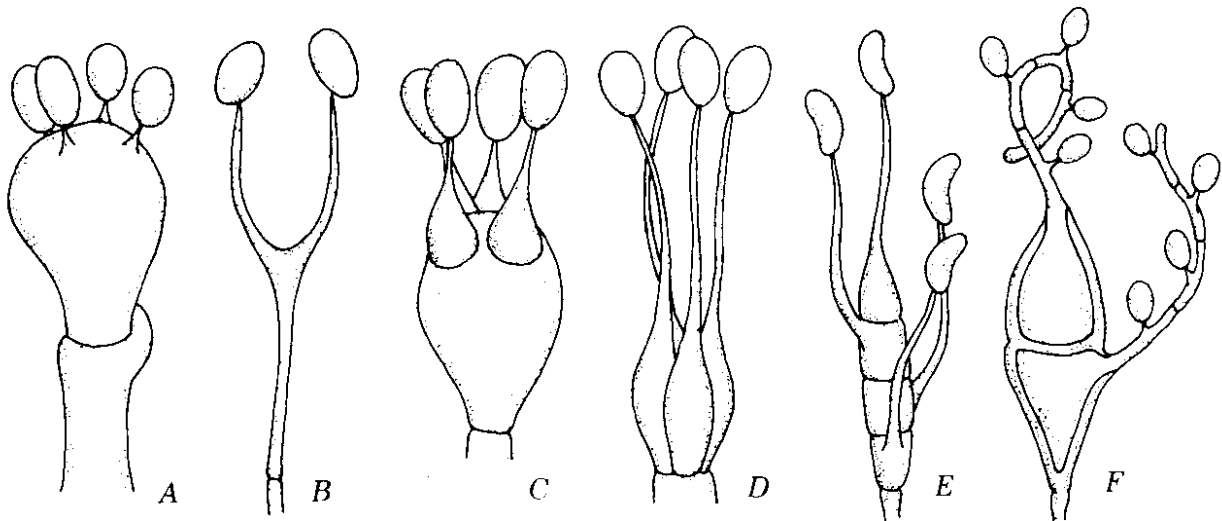
**Figure 14.** Deposit of abundant of spores along the inner side of the tubes in *Trametes versicolor*. The majority of the spores travel only 0.2-0.3 mm horizontally after they are discharged from the basidia (red arrow). Bar = 0.1 mm.



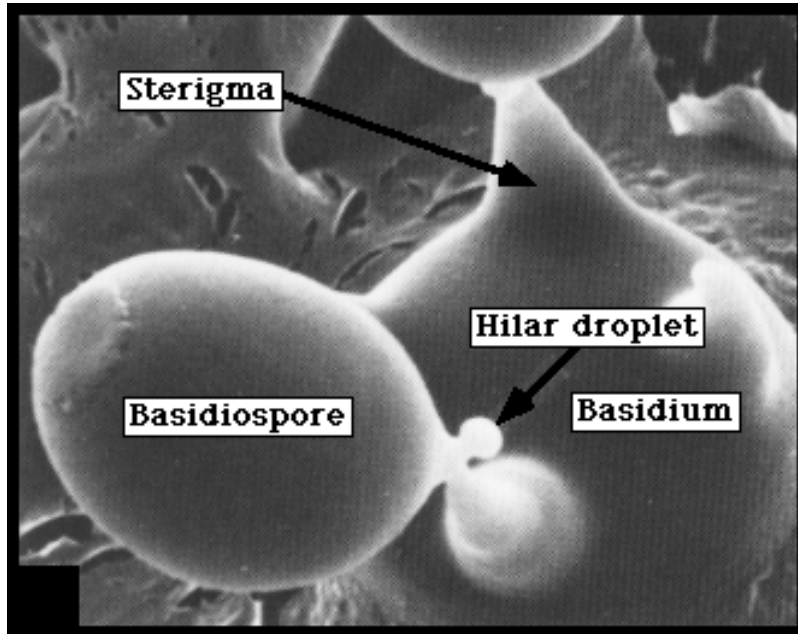
**Appendix A.** Development of a typical basidium. Meiosis occurs in the swollen basidium results in four nuclei. Sterigmata initiate on the apex of the basidium, followed by the formation of basidiospores. Migration of nuclei through sterigmata to basidiospores produces uninucleate basidiospores (Alexopoulos, *et al.*, 1996).



**Appendix B.** Different types of mature basidia. (A) typical holobasidium; (B) holobasidium bearing only two sterigmata and basidiospores; (C) basidium with swollen sterigmata; (D) phragmobasidium with longitudinal septa and with extremely long sterigmata; (E) phragmobasidium with transverse septa separating individual cells of the metabasidium; (F) basidium of *Puccinia* (Alexopoulos, *et al.*, 1996).



**Appendix C.** Scanning electron micrograph showing the structure of a ballistosporic basidiospore with developing Buller's drop in species *Coprinus cinereus*: Agaricomycotina (McLaughlin *et al.*, 1985).



## Appendix D.

Subdivision:

Basidiomycotina

Subclass: Holobasidiomycetidae

(Homobasidiomycete Fungi)

(substantial mushrooms)

Order: Agaricales

Family: Agaricaceae

Family: Bolbitiaceae

Family: Clavariaceae

Family: Coprinaceae

Family: Cortinariaceae

Family: Entolomataceae

Family: Hydnangiaceae

Family: Lycoperdaceae

Family: Marasmiaceae

Family: Nidulariaceae

Family: Pleurotaceae

Family: Pluteaceae

Family: Schizophyllaceae

Family: Strophariaceae

Family: Tricholomataceae

Order: Boletales

Family: Boletaceae

Family: Boletinellaceae

Family: Coniophoraceae

Family: Calostomataceae

Family: Gyrodontaceae

Family: Paxillaceae

Family: Rhizopogonaceae

Family: Sclerodermataceae

Family: Suillaceae

Order: Cantharellales

Family: Cantharellaceae

Family: Clavulinaceae

Family: Hydnaceae

Order: Dacrymycetales

Family: Dacrymycetales

Order: Gomphales

Family: Gomphaceae

Family: Hysterangiaceae

Family: Phallaceae

Family: Ramariaceae  
Family: Sphaerobolaceae

Order: Hymenochaetales

Family: Hymenochaetaceae

Order: Polyporales

Family: Atheliaceae  
Family: Ganodermataceae  
Family: Gloeophyllaceae  
Family: Meripilaceae  
Family: Podoscyphaceae  
Family: Polyporaceae  
Family: Steccherinaceae

Order: Russulales

Family: Auriscalpiaceae  
Family: Corticiaceae  
Family: Hericiaceae  
Family: Meruliaceae  
Family: Rusulaceae  
Family: Stereaceae

Order: Thelephorales

Family: Bankeraceae  
Family: Thelephoraceae

Subclass: Phragmobasidiomycetidae  
(Heterobasidiomycete Fungi)

Order: Auriculariales

Family: Auriculariaceae

Order: Tremellales

Family: Exidiaceae  
Family: Tremellaceae  
Family: Tremellodendropsidaceae